5-2019

Thousand Cankers Disease Diagnosis with Conventional Electrophoresis and TaqMan Probes

Tammy Lynn Stackhouse
University of Tennessee, tstackho@vols.utk.edu

To the Graduate Council:

I am submitting herewith a thesis written by Tammy Lynn Stackhouse entitled "Thousand Cankers Disease Diagnosis with Conventional Electrophoresis and TaqMan Probes." I have examined the final electronic copy of this thesis for form and content and recommend that it be accepted in partial fulfillment of the requirements for the degree of Master of Science, with a major in Plant Sciences.

William E. Klingeman III, Major Professor

We have read this thesis and recommend its acceptance:

Denita Hadziabdic-Guerry, Robert N. Trigiano

Accepted for the Council:
Dixie L. Thompson

Vice Provost and Dean of the Graduate School

(Original signatures are on file with official student records.)

Thousand Cankers Disease Diagnosis with Conventional Electrophoresis and TaqMan Probes

A Thesis Presented for the
Master of Science
Degree
The University of Tennessee, Knoxville

Tammy Lynn Stackhouse
May 2019

Acknowledgements

I would like to thank my major professor, Dr. William Klingeman, for his guidance and encouragement throughout this research project. Without his mentorship, support, and hours of editing I would not have completed my thesis. I would also like to thank my committee members, Dr. Denita Hadziabdic and Dr. Robert Trigiano. Both welcomed me into their lab groups and allowed use of their lab equipment. They also were essential in ensuring the completion of this project, through both their expertise and enthusiasm. I could not have asked for a better group of individuals to lead me on this journey.

I would also like to thank Sarah Boggess and Sujata Agarwal for their guidance in the laboratory. Both saved me from many nights pulling my hair out over confusing results. My fellow labmates, Dr. Grace Pietsch, Meher Ony, Beant Kapoor, and Nick Strange, thank you for your friendship and support. May your coffee pot never run dry and your research always thrive.

Thank you to the United States Forestry Service (18-DG-11132544-011) for the financial support of this research project. Without grants like these, research could not move forward.
I'd like to give a special thanks to both the Plant Sciences and Entomology and Plant Pathology departments of the University of Tennessee. Both have been home for me since my undergraduate years and I wouldn't be the same person without each faculty, staff, and student I encountered.

Finally, I'd like to thank my mother, Natalie Harris, and partner, Brock Taylor, for their emotional support throughout the years. Graduate research was a challenge, but these two always supported me every step of the way.

Abstract

Juglans nigra and related *Juglans* and *Pterocarya* species of trees are threatened by the fungus *Geosmithia morbida,* and the bark beetle *Pityophthorus juglandis* that serves as the primary vector for the plant pathogen. Together, this species complex causes thousand cankers disease (TCD) in susceptible host plants. When infection is severe, tree death can occur within three to four years, resulting in severe ecological and economic damage. Although the previously developed TCD rapid detection molecular protocol can quickly identify the presence of the vector or the pathogen, it requires specialized and costly equipment, and highly trained personnel. To make this protocol more user friendly this study aims to 1) to optimize the current molecular protocol by evaluating the lowest detection limits of *G. morbida* and *P. juglandis* on a conventional gel and 2) reduce the materials and equipment costs associated with the PCR result through a direct visualization method. As a result, reliance on the QIAxcel Advanced capillary electrophoresis system has been negated, and replaced by more affordable diagnostic methods, which included either conventional agarose gels or molecular probe protocols. The expensive QIAxcel Advanced capillary electrophoresis system (costing several tens of thousands of dollars US) was replaced with two less substantial costs; a $3,000 piece of equipment in the conventional gel protocol or a $200 piece of equipment in the molecular probe assay. Both the conventional gel and molecular probe protocols successfully detected the presence of the fungal and insect components of the disease. These new protocols will make the testing of *J. nigra* samples more accessible to regulators and diagnosticians.

Table of Contents

List of Figures

List of Tables

1 Introduction

Thousand Cankers Disease

Thousand cankers disease (TCD) is a disease complex that affects walnut/butternut (*Juglans* spp. L.) (Tisserat et al., 2009; Kolařík et al., 2011; Serdani et al., 2013; Seybold et al., 2013b) and wingnut host plant species (*Pterocarya* spp. Nutt. ex Moq.) (Hishinuma et al., 2016). TCD results from the fungus *Geosmithia morbida* Kolarik, Freeland, Utley, and Tisserat (Kolařík et al., 2011; Utley et al., 2013) being spread to susceptible host plants by its principal bark beetle vector, *Pityophthorus juglandis* Blackman (Coleoptera: Curculionidae: Scolytinae), walnut twig beetle (WTB) (Seybold et al., 2013b; Rugman-Jones et al., 2015). Between the mid-1990s and 2001, ornamentally grown eastern black walnut (*J. nigra*) progressively declined in Oregon and Colorado without explanation (Tisserat et al., 2009; Tisserat et al., 2011). By 2008, *P. juglandis* was identified as the vector for a fungal species responsible for TCD for which *G. morbida* is the principal plant pathogen (Tisserat et al., 2009). The disease was named "thousand cankers disease" after the series of coalescing cankers in the phloem of the trees where *P. juglandis* had been active (Tisserat et al., 2009; Kolařík et al., 2011).

Host Plant Species to Thousand Cankers Disease

Juglans is a temperate genus comprised mostly of hardwood trees and with 16 species occurring in North and South America. Six of these species are found within the continental United States (Stone et al., 2009). All *Juglans* spp. can be infected with TCD, but *J. nigra* is the most susceptible (Tisserat et al., 2009; Utley et al., 2013; Seybold et al., 2019). *Juglans nigra* is indigenous from Minnesota to Florida, and from the Atlantic coast to Texas but tree growth is sparse within the Mississippi River Valley (Williams, 1990). *Juglans nigra* growth is not evenly distributed in its range, but instead occurs in high densities in Missouri, Ohio, and Kentucky

(Williams, 1990). Individual *J. nigra* trees typically grow alone or in small clusters in forested areas (Williams, 1990; Randolph et al., 2013). This species requires deep, well-draining soils, and with an average annual temperature around 13^{o}C, and annual precipitation of 890 mm or more (Goodell, 1984; Barnes and Spurr, 1998).

Juglans nigra has important environmental and economical roles in its native and nonnative regions. It is a wildlife food resource for forest rodents, especially in years that acorn production is low (Grant et al., 2011; Seybold et al., 2019). Beyond the wildlife impact, *J. nigra* also adds to species richness in the forests (Grant et al., 2011; Daniels et al., 2016), as well as *J. nigra* food for human consumption, veneer, timber, oils, and extracts (Newton and Fowler, 2009; Leslie et al., 2010; Seybold et al., 2019). The wood is highly prized for its physical and mechanical properties and provides a high-value lumber used for furniture (Goodell, 1984; Voulgaridis and Vassiliou, 2005). *Juglans nigra* is now found throughout the United States because of its use as an ornamental crop and as scions for *J. regia* L. (English walnut). As a scion, it protects against extreme cold and soilborne pathogens, such as *Agrobacterium tumefaciens* Smith and Townsend (crown gall) and root rot caused by *Phytophthora* spp. de Bary (Nguyen, 2015; Bernard et al., 2018).

The decline of *J. nigra* would result in serious economic impacts on food, medical, and industrial trade associated with this species (Grant et al., 2011). The standing value of *J. nigra* within its native range is over $539 billion and represents 96 million cubic board meters of lumber (Newton and Fowler, 2009; Randolph et al., 2013). In Tennessee, the value of *J. nigra* is estimated at $1.47 billion in forested areas and $1.37 billion in urban areas (Haun et al., 2010). The effects of thousand cankers disease could have a serious impact on forests and economics throughout the United States. *Juglans* species are highly susceptible to TCD and, coupled with

the ease of *G. morbida* and *P. juglandis* movement with timber, could lead to massive tree die-offs and possible regional extinction (Utley et al., 2013). The decline of *J. nigra* in public and private landscapes could lead to higher costs for tree removal for homeowners, with an estimated cost of $150 to $1,200 per tree (Newton and Fowler, 2009; Grant et al., 2011; Lauritzen, 2018; Seybold et al., 2019).

The Principal Insect Vector of TCD

The principal vector of *G. morbida* is a beetle, *P. juglandis.* The beetle is light brown, 1.5-1.9 mm long, and originally found in New Mexico and Arizona in 1928 (Bright, 1981). The beetle was later discovered in Northern Mexico and California in 1959 (Bright, 1981; Wood, 1982; Seybold et al., 2016). The primary host of *P. juglandis* was the Arizona walnut (*J. major* (Torr.) A. Heller) with the California walnut (*J. californica* S. Watson) being a potential host in overlapping areas (Seybold et al., 2012). *Pityophthorus juglandis* have now been collected from six *Juglans* species (Leslie et al., 2010; Seybold et al., 2012). The expansion of the range of *P. juglandis* may have occurred via beetle flights but, given the typical flight range of about 3 kilometers, human-mediated movement likely transported the species to eastern United States (Newton and Fowler, 2009; Hadziabdic et al., 2014a; Rugman-Jones et al., 2015) and to Italy (Montecchio et al., 2016; Moricca et al., 2018). The beetle can easily be moved from one place to another via timber during processing (Seybold et al., 2019).

Pityophthorus juglandis can reside in a variety of environmental conditions, which can help establish further spread of the species into new areas (Grant et al., 2011; Hadziabdic et al., 2014a; Zerillo et al., 2014; Hefty, 2016). In recent years, the western range of *P. juglandis* has expanded into Colorado, Idaho, Nevada, Utah, and Washington (Tisserat et al., 2011; Thousandcankers.com, 2017). *Pityophthorus juglandis* was first found in Knoxville, TN in 2010

with its vectored pathogen, *G. morbida* (Grant et al., 2011). Since then, *P. juglandis* has been found and wood movement has been quarantined in Pennsylvania (2011), Virginia (2011), Ohio (2013), and Maryland (2014) (Hansen et al., 2011; Fisher et al., 2013; maryland.gov, 2018). Both *P. juglandis* and *G. morbida* have also been found on *J. nigra* and *J. regia* in northern Italy in 2013 and central Italy in 2018 (Montecchio and Faccoli, 2014; Montecchio et al., 2016; Moricca et al., 2018). The further spread of thousand cankers disease to Europe could be disastrous due to the high economic value of both *J. nigra* wood and fruit within Italy (Moricca et al., 2018).

While thousand cankers disease produces dieback in the base of twigs, *P. juglandis* are active and have been found in and around above ground portions of the tree (Grant et al., 2011; Klingeman et al., 2017). The adults and larvae overwinter in trees and adults emerge between January and March (Nix, 2013). Females lay eggs in horizontal tunnels or galleries in the cambial layer (Nix, 2013). Larvae then tunnel vertically in the phloem, leaving galleries that are between 2.5 and 5 cm long (Seybold et al., 2013a). *Pityophthorus juglandis* enter and exit the tree through pinhead-sized holes that are about 0.64-0.75 mm across (Graves et al., 2009). Unlike many other fungal-associated insects, *P. juglandis* do not have mycangia (Newton and Fowler, 2009; Nguyen, 2015). Without this special organ for transporting fungi, *P. juglandis* carry *G. morbida* externally and potentially internally (Newton and Fowler, 2009). The beetles deposit the fungus spores while burrowing.

Pityophthorus juglandis can be captured using pheromone traps or with *G. morbida* and *Juglans* spp. volatile organic compounds (VOCs) for identification (Seybold et al., 2013b; Hadziabdic et al., 2014b; Blood et al., 2018). While two generations of beetles a year is most common, three generations of *P. juglandis* may be possible in milder climates allowing for rapid population increases (Tisserat et al., 2009; Freeland et al., 2012).

The Pathogen Causing Thousand Cankers Disease

Geosmithia morbida is an asexual reproducing, filamentous ascomycete fungus that causes thousand cankers disease (TCD) (Kolařík et al., 2011). While *G. morbida* sporulates on the bark surface and could possibly be spread by wind or water, it is most effectively disseminated by an insect vector (Kolařík et al., 2008; Tisserat et al., 2009; Hadziabdic et al., 2014a; Zerillo et al., 2014). The pathogen has not been found to be systemic within the tree, and instead, is found in and around the *P. juglandis* tunnels (Newton and Fowler, 2009). Without the aid of dispersal by the principal beetle vector, the pathogen typically does not establish well in trees (Newton and Fowler, 2009; Hadziabdic et al., 2014a; Nguyen, 2015). Although there is limited research available regarding pathogenicity of *G. morbida* (Schuelke et al., 2017), Chahal (2017) found that virulence can vary greatly between different strains of *G. morbida* (Chahal, 2017; Chahal, in preparation).

The genome of *G. morbida* is diverse, but relatively small; around 26.5 Mbp (Schuelke et al., 2016). The genome contains about 6000 genes with less than one percent repetition (Schuelke et al., 2016). Based on the size of its genome and pathogenicity differences from other *Geosmithia* spp., it may have a unique evolutionary path making its pathogenicity different that other plant-associated fungi (Schuelke et al., 2017). Current data supports the hypothesis that *G. morbida* evolved alongside *P. juglandis* and *J. major,* and possibly *J. californica* and *J. hindsii* (Jeps.) Jeps. ex R. E. Smith, however not *J. nigra* (Kolařík et al., 2011) (Williams, 1990; Hadziabdic et al., 2014a). This can make *G. morbida* a huge risk to *J. nigra* and other *Juglans* spp. because of the absence of co-evolutional encounters with the disease due to geographic distance of the tree and pathogen (Tsui et al., 2012; Hadziabdic et al., 2014a).

Geosmithia morbida has been found with other beetle species in addition to its principal vector, *P. juglandis* (Ginzel and Juzwik, 2014; Juzwik et al., 2016; Chahal, 2017). With time and sufficient sampling, *G. morbida* has generally been found wherever new occurrences of *P. juglandis* are detected. This spread of *G. morbida* via its principal vector has allowed TCD to become widespread throughout the United States, in addition to parts of Mexico and Italy (Montecchio et al., 2016; USDA-FS-PPQ, 2018). However, *G. morbida* has also been found in North Carolina without its beetle vector (Hadziabdic et al., 2014b). It is possible that the beetles were present but not captured, and entrance and exit holes were not observed. *Geosmithia morbida* was also found in Indiana without its traditional vector and was instead found on the weevil *Stenomimus pallidus* Boheman (Ginzel and Juzwik, 2014). In Indiana, 435 *S. pallidus* adult beetles were collected, but *G. morbida* was recovered on only three individuals. The low number of beetles carrying the pathogen suggests the need for better detection methods, or may indicate that the relationship between these two species may be casual, thus not likely to result in appreciable damage to *J. nigra* (Ginzel and Juzwik, 2014). In 2016, two ambrosia beetles, *Xylosandrus crassiusculus* (Motchulsky) and *Xyleborinus saxesenii* (Ratzeburg), were added to the list of beetle species able to carry *G. morbida* on their bodies (Juzwik et al., 2016). These beetles were collected from TCD-infected trees and it is probable that the pathogen was transferred following interaction with *G. morbida* occurring in or adjacent to *P. juglandis* galleries. Work by Chahal et al (in preparation) expands this list to include eleven beetle species, which raises concerns that alternative vectors may be potential actors in spreading TCD or sustaining infection where TCD occurs (Chahal, 2017; Chahal, in preparation).

There are several challenges in detecting *G. morbida* within a branch sample submitted for diagnostic evaluation. *Geosmithia morbida* is difficult to isolate and is easily outcompeted in

culture because of its slow growth habit (McDermott-Kubeczko, 2016). Growing a colony on culture plates requires multiple re-isolations to obtain axenic cultures, and there are no species-specific media available (Oren et al., 2018). This process typically requires two to six weeks because of the slow-growing nature of the species and still necessitates microscopic identification from trained personnel (Oren et al., 2018).

Thousand Cankers Disease Symptoms and Challenges for Treating Infected Host Plants

Thousand cankers disease can be extremely difficult to diagnose (Oren et al., 2018). The symptoms are often confused with drought stress as both can cause wilting and yellowing of the leaves, branch dieback, and crown thinning (Seybold et al., 2013b). The bark of infested trees must be removed to identify dark-brown to black cankers located in in the phloem and cambium area (Newton and Fowler, 2009; USDA-FS-PPQ, 2018). As disease progresses, the cankers can coalesce and create large necrotic areas that girdle the tree over time (Tisserat et al., 2009; Seybold et al., 2013b). Numerous cankers as a result of *G. morbida* infestations destroys the phloem and cambium of the tree, which can cause nutrient depletion and ultimately tree mortality (Graves et al., 2009; Seybold et al., 2013b; Seybold et al., 2019). The vector, *P. juglandis*, creates a pinhole-sized entrance and exit holes on the bark, but can easily be missed or confused with other potential vectors (Seybold et al., 2013b; Hadziabdic et al., 2014a; USDA-FS-PPQ, 2018). In *J. nigra*, thousand cankers disease can cause tree mortality within three to four years following appearance of the original symptoms. Therefore, early identification is critical for limiting spread of the insect and disease via regulatory efforts (Kolařík et al., 2011; Hadziabdic et al., 2014a). Some species, such as *J. regia* and *J. major* that are suspected of

coevolving with *P. juglandis* and *G. morbida*, can survive with thousand cankers disease for much longer periods (Seybold et al., 2019).

There are currently no viable pesticide treatment options available for thousand cankers disease. Chemical insecticidal treatments have limited efficacy and should only be used on high value timber (Haun et al., 2010; Freeland, 2012). Insecticidal controls that may work to control the beetle, such as imidacloprid and dinotefuran, are not allowable on food crops given current pesticide labeling (Nix, 2013; Paul et al., 2013). Neonicotinoids are also attributed with harm to honey bees, bumble bees, and other insect pollinators, so often are avoided for that reason (Whitehorn et al., 2012). The current method used to control spread of thousand cankers disease is regulatory quarantine, which only allows the wood to leave an infested area after a processing treatment, such as a heat treatment, chemical treatment, or kiln-drying of wood, has been applied (Mayfield et al., 2014; Audley et al., 2015; Audley et al., 2016). Treated wood with intact bark may still present risk of spreading the disease, so additional processing and storage steps for that wood may be required. Current studies suggest that kiln-dried or permethrin-treated wood is not likely to become re-infested after treatment, where steam treatments have not been sufficient to prevent re-infestation (Audley et al., 2015; Audley et al., 2016; Mayfield et al., 2018). If a treatment does not kill the pest, the wood should be destroyed to prevent pest spread (Haun et al., 2010; Freeland et al., 2012). As of 2016, *P. juglandis* has been identified from 23 counties in Tennessee, and ten counties are quarantined for thousand cankers disease (Hefty et al., 2016; TN.gov, 2018; Seybold et al., 2019).

A Molecular Protocol for TCD Identification: Examining the Oren et al. 2018 Study

To prevent further spread of thousand cankers disease, pathogen identification tests must be performed on drilled bark shaving samples to confirm disease presence and enforce

quarantine for infested counties. Eastern strains of *G. morbida* have been difficult to isolate, grow slowly under laboratory conditions, and thus take more time to diagnose (Gazis et al., 2018). In addition, *P. juglandis* traps have a limited range of efficacy across which they can reliably attract beetles from nearby *J. nigra* trees (Nix, 2013; Oren et al., 2018). These obstacles have made timely disease identification difficult. These challenges can be overcome by using molecular methods to test for the presence of the beetle and/or pathogen in submitted host plant branch samples. Currently, *G. morbida* and *P. juglandis* can be identified using the QIAxcel Advanced capillary electrophoresis system a polymerase chain reaction (PCR) protocol using species-specific microsatellite loci (Oren et al., 2018). This protocol allows for drilled bark shaving samples to be checked for the presence or absence of the beetle and pathogen quickly and relatively easily.

PCR has been utilized for disease diagnosis for many plant, human, and animal diseases (Hamelin et al., 2000; Versalovic and Lupski, 2002; Silva et al., 2016). Molecular methods allow for detection of minute amounts of DNA with a drastically reduced amount of time compared to growing up fungi in culture (Cawkwell et al., 1993; Lamarche et al., 2015). Assuming proper optimization, PCR is a process of sample amplification only if the template DNA matches the primers. PCR is sensitive enough to select DNA that matches its specific primers even if there is a non-target DNA present (Saiki et al., 1988). The primers used in the Oren et al. (2018) study are species specific and were tested against various other closely related pathogen and beetle species. PCR products can, in some cases, be visualized with agarose gel, and in other cases have needed a more sophisticated system (e.g., a QIAxcel Advanced capillary electrophoresis system) (Oren et al., 2018).

Microsatellites, otherwise known as simple sequence repeats (SSRs), are repeated motifs found in the genomes of eukaryotes (Zane et al., 2002). These patterns are typically 1-6 base pairs long and repeat at least several times in tandem. Microsatellites are found in coding and noncoding regions and can often have length as well as compositional polymorphisms (Schlötterer and Tautz, 1992; Zane et al., 2002). DNA replication is not an error-free process and often introduces mutations into a sequence because of slippage, particularly in areas of DNA with repeating sequences (Schlötterer and Tautz, 1992). This slippage allows the number of times a microsatellite motif is repeated in a sequence to vary between individuals. The high variability in microsatellites makes them powerful genome mapping tools. While the motifs are extremely variable, the flanking regions associated with them are typically highly conserved (Lench et al., 1996; Zane et al., 2002). Conservation of flanking sequences between individuals allows the creation of species-specific primers (Hadziabdic et al., 2012; Hadziabdic et al., 2015).

The PCR-based molecular protocol for identifying *G. morbida* identification of TCD was developed using samples collected from infestations in California and Tennessee. In addition, wood samples from Missouri were tested as a negative control (Oren et al., 2018). Branches from forty trees from each above-mentioned areas were collected resulting in 1,600 samples that were further analyzed for the presence of *G. morbida* and *P. juglandis*. Drilled bark shaving samples were collected using the following two different methods: 1) by peeling the bark to expose necrotic areas to drill (lesion directed), or 2) direct drilling into the bark (feature directed). The second, feature directed method, was used to mimic insect activity found on the branches, or any other natural opening such as lenticels, secondary branch unions, bark furrows, and wound sites (Oren et al., 2018).

The PCR results of the 1600 samples in the Oren et al. study (2018) detected the disease in 85% of California samples, 42.5% of Tennessee samples, and 0% in the Missouri (negative control) samples. Independent of labor inputs, the materials costs associated of collecting a sample using this strategy is currently about $10.60. This protocol was highly specific and sensitive, while drastically reducing sample processing time and effort. Unfortunately, the practicality of end user adoption is limited, in part because the protocol requires specialized, expensive equipment, and user training or expertise.

Project Research Needs and Key Objectives

There is a critical need to refine the Oren (2018) PCR protocol to make it more user friendly and understand its limits before the protocol can be utilized in diagnostic labs throughout the United States and Europe. This study aims to develop molecular tools that can be simplified, compared to the currently available protocol, and that are cheaper and available for use with conventional electrophoresis. For this project, we propose the following objectives: 1) to optimize the existing thousand cankers disease PCR diagnostic protocol for use with conventional electrophoresis, and 2) to develop a novel toolkit for rapid diagnosis using molecular probes. Using findings obtained in this study we will clearly define the least amount of pathogen or beetle DNA necessary to yield a positive reading, and simplify the process for diagnosis. The result of this research will be a protocol that can be utilized by municipal arborists, urban foresters, regulatory agents, and diagnosticians that requires as little time and laboratory equipment inputs as possible.

2 Thousand Cankers Disease Identification Using Conventional Electrophoresis

2.1 Abstract

Juglans nigra is native throughout the eastern United States and used in the western United States both as a rootstock with *J. regia* and as an ornamental plant. *Juglans nigra* is a timber crop and food source for both humans and wildlife in its native habitats, and estimated to be worth over 539 billion dollars (USD) in its native range alone. However, this important tree is threatened by the thousand cankers disease complex. This complex is formed by *Pityophthorus juglandis*, a bark beetle, and *Geosmithia morbida*, the fungal pathogen. Together, the bark beetle and fungus form necrotic cankers within susceptible hosts, *Juglans* and *Pterocarya* species. The disease can kill a *J. nigra* tree within four years. To test the presence of this disease, a molecular tool was developed to identify *G. morbida* and *P. juglandis*, but required a QIAxcel Advanced capillary electrophoresis system that can cost in tens of thousands of dollars (US). Results from this research removes need for the QIAxcel Advanced capillary electrophoresis system in the protocol and instead, a conventional gel protocol can be used to reduce the costs associated with equipment. This protocol successfully assayed *G. morbida* and *P. juglandis* DNA from drilled bark shaving samples and bark sample constructs. Assays were also performed to determine the sensitivity of the new conventional gel protocol, which was capable of detecteing target species DNA to as low as seven hyphal or conidia cellular equivalents based on genome copy number calculations. The affordability and simplicity of this modified protocol will enable more rapid adoption by regulators and diagnosticians.

2.2 Introduction

Thousand cankers disease (TCD) is a complex disease involving a susceptible host tree, an insect vector, and a fungus. Susceptible host trees include species of *Juglans* spp. L. (walnut and butternut trees) or *Pterocarya* spp. Nutt. ex Moq. (wingnut) (Tisserat et al., 2009; Kolařík et

al., 2011; Hishinuma et al., 2016). The principal bark beetle vector, *Pityophthorus juglandis* Blackman, can be found in the thousands per tree in areas of heavy infestation (Nguyen, 2015). Beetle larvae create galleries by feeding on phloem and cambial tissues of tree branches and the main trunk, where transmitting the infectious fungal pathogen, *Geosmithia morbida* Kolarik, Freeland, Utley, and Tisserat forms the cankers (Tisserat et al., 2009; Kolařík et al., 2011; Seybold et al., 2013a; Rugman-Jones et al., 2015). As the pathogen grows, necrotic cankers coalesce and can eventually girdle and kill the tree (Tisserat et al., 2009). This disease complex, which has been found throughout the western United States, several states in the eastern United States, and parts of Italy, can cause tree decline and death in as little as three to four years (Nix, 2013). This pathogen has traditionally been difficult to identify from host symptoms that may be observed in the field, because most visible TCD-associated symptoms, such as wilting leaves and early dieback, are similar drought stress symptoms *Juglans* spp. (Seybold et al., 2019). Accurate diagnosis of the cause of injury generally involves closer examination of signs and symptoms that may only be visible beneath the bark (Seybold et al., 2013a). Even if the bark is removed and cankers or lesions are present, it can take six weeks or more to accurately confirm the fungi through non-molecular means such as agar culturing (Oren et al., 2018). The effects of this pathogen can be devastating for orchard, timber stands, and urban areas with *J. nigra* (Seybold et al., 2019).

An identification technique using a molecular protocol was introduced in 2018 that uses Polymerase Chain Reaction (PCR) to target microsatellite regions (Oren et al., 2018). This protocol was developed with *J. nigra* and *J. hindsii* samples collected in California, Tennessee, and Missouri and used to test for presence of *G. morbida* and *P. juglandis* DNA. The existing protocol (Oren et al. 2018) has removed need by the identifier to grow and subculture a fungal

isolate, which reduces time associated with the identification step from six weeks, to possibility of confirmation of the pathogen and beetle within about one day. However, the efficiency and adaptability of the molecular protocol is constrained by requirements for advanced user expertise and expensive equipment. A need remains to optimize this protocol and to seek methodologies that can be adapted to meet cost constraints and technical capabilities of municipal arborists, urban foresters, regulatory agents, and clinical diagnosticians.

PCR is a molecular protocol that is used across scientific disciplines that helps to determine if a specific DNA sequence is present in a sample (Saiki et al., 1988). PCR requires a master mix that includes the following components: a thermostable polymerase, primers, deoxyribonucleotide triphosphates (dNTPs), template DNA, magnesium, and a buffer. Extra ingredients, such as DMSO, may be added to increase efficiency before placing the mix in a thermocycler, a machine designed to cycle through specific regimen of temperatures in quick succession. The mix containing template DNA and master mix is placed at a very high temperature, around 94-96ºC, to denature the template DNA, then a lower temperature, around 55-60ºC, to allow the primers to anneal to complementary DNA. Primers used in this process are often 20-30 bp sequences that match the template DNA at a specific location in the target genome's sequence (Oren et al., 2018). If the primers are complementary to that sequence then they will anneal, if not then the primers remain unattached, resulting in no amplification and no bands showing up on a gel. After annealing, the temperature is raised to approximately 72ºC and the polymerase attaches near the primers at which time it begins adding dNTPs to create a second complementary strand of DNA. This cyclic process is repeated between 30 and 40 times, with each cycle increasing the number of target DNA copies at a near exponential rate, until components are exhausted. The whole process takes between 30 minutes and 2 hours. The

product is short sequences of a known, specific base-pair length. Products are separated using automated or conventional gel systems and visualized with either a fluorescent compound, which intercalates into target DNA, or with a fluorochrome incorporated into a probe.

Gel systems allow for visualization of a PCR product by separating by size the DNA within a sample. The gel itself is a porous semisolid matrix that DNA can move through when electricity is applied (Smejkal and Lazarev, 2006). This process works by putting samples into wells (small indentations) in a 2% gel submerged in 1X TAE buffer and running a current through the buffer. The DNA is negatively charged and therefore is drawn through the gel matrix towards the positive cathode. Smaller DNA fragments can move through the gel faster, while larger fragments take more time (Smejkal and Lazarev, 2006). A DNA ladder is added to a gel along with the samples to establish bands of pre-determined sizes for later visualization. A fluorescent dye is added to the DNA before running the samples. This dye binds to the double-stranding DNA and will fluoresce under a specific wavelength, allowing the bands to be visualized. By comparing a sample to the DNA ladder one can determine the size of a fragment made by a PCR reaction. Negative reactions will not have amplified during PCR and therefore will not have bands.

There are two common gel systems: conventional and automated. While premade conventional gels can be ordered, typically a gel is produced by combining agarose and buffer in a beaker, heating up these ingredients, adding a dye, pouring the product into a mold, and then waiting for the gel to solidify at room temperature before use. Another option is to use automated gel systems, such as the QIAxcel Advanced capillary electrophoresis system, which only requires the user to add the samples to the machine and wait for an output of bands in a digital gel format.

There are a few key differences between a QIAxcel Advanced capillary electrophoresis system and a conventional gel system. The QIAxcel Advanced capillary electrophoresis system uses an acrylamide gel with uniform pore size, which is fixed vertically within the machine, has a very high resolving power for small fragments. A conventional gel is typically an agarose gel-horizontally run, with lower resolution for small fragments, has non-uniform pore size, and the gel may not set evenly every time. The QIAxcel Advanced capillary electrophoresis system uses a premade cartridge that contains the gels, eliminating the need for a user to make them, but increasing the total operational cost. Using the QIAxcel Advanced capillary electrophoresis system is relatively easy to use but it does require specialized training and is expensive, thus unobtainable for most small diagnostic labs.

The objectives of this study were to adapt the Oren et al. (2018) protocol by optimizing inputs and procedures that can enable adaptation for use with a conventional gel system. Optimization steps involved assessment of the detection capability for the PCR protocol. Sample accessions included testing with microsatellite primers designed to detect DNA from: 1) *G. morbida* pure culture; 2) *P. juglandis* species; 3) drilled bark shaving samples assayed in Oren et al. (2018) that tested positive for *G. morbida* DNA, 4) drilled bark shaving samples assayed in Oren et al. (2018) that tested positive for *P. juglandis* DNA, 5) bark sample constructs that tested positive for *G. morbida* DNA, and 6) bark sample constructs positive for *P. juglandis* DNA. The improved procedures are expected to make testing for *G. morbida* and *P. juglandis* species significantly less expensive than the protocol constrained by equipment necessary to run using specialized equipment such as QIAxcel Advanced capillary electrophoresis system or qPCR (real-time polymerase chain reaction) system. In addition, these improvements would enable running samples in less time and with shorter training for the end user. For example,

conventional gels are more widely used than automated systems, including ongoing training and use in some high school science laboratories.

2.3 Materials and Methods

Extractions procedures for *Geosmithia morbida* and *Pityophthorus juglandis* DNA

The QIAamp Fast DNA Stool Mini Kit (Qiagen, Germantown, MD, USA) was used per the manufacturer's protocol to extract *G. morbida* fungal DNA taken from mycelia grown in axenic cultures (DNA type 1, Table 2.1) and *P. juglandis* DNA extracted from whole beetles (DNA type 2, Table 2.1). A NanoDrop Microvolume Spectrophotometer (ThermoFisher, Waltham, MA, USA) was used to determine the concentrations of *G. morbida* and *P. juglandis* DNA that were present within each sample.

Drilled Bark Shaving Sample DNA Extraction Protocol

This assay utilized the DNA extracted previously from the drilled bark shaving samples taken in the Oren et al. (2018) study. The drilled bark shaving samples were collected as described by Oren et al. (2018) using lesion-directed drilling. Briefly, portions of the bark (phloem) was removed from branch pieces taken from *J. hindsii* (CA) and *J. nigra* (MO and TN) trees using with a sterilized scalpel to reveal cankers, lesions, and discoloration of the phloem tissues. A drill bit was put through a microfunnel (bottomless microcentrifuge tube) then the cankers were drilled. The drilled bark shaving samples contained mostly phloem and some wood tissues, were collected within the microfunnel, and then transferred into a 1.5 microcentrifuge tube. After each use the drill bits and scalpel were sterilized with a bead sterilizer (Steri 350, Fisher Scientific, Pittsburgh, PA, USA), and 70% non-denatured ethanol was used to clean work surfaces between samples. These tubes were kept at -20ºC until the samples were processed. A

QIAmp Fast DNA Stool Mini Kit (Qiagen, Germantown, MD, USA) was used following the manufacturer's protocol to extract DNA from the drilled bark shaving samples.

PCR Protocol (Oren et al. 2018)

PCR reactions contained 1 µL DNA (concentration varies), 4 µL Go-Taq G2 Hot Start Colorless Master Mix (Promega, Madison, WI, USA), 1 µL of each primer, 0.5 µL dimethyl sulfoxide (DMSO), and 2.5 µL of sterile water 10 µL volume. PCR runs used in both conventional and automated gel systems were doubled to a 20 µL volume. Each run included a positive DNA control, which consisted of DNA extracted from an axenic *G. morbida* culture and *P. juglandis* beetle tissues, and a negative control of sterile water. PCR was run using a SimpliAmp™ Thermal Cycler (Applied Biosystems, Foster City, CA, USA) in 96-well plates. The thermocycler was set to an initial denaturation step of 3 minutes at 94ºC, then 35 cycles of 94ºC for 40 seconds, 55ºC for 40 seconds, and 72ºC for 30 seconds, followed by a final extension of 72ºC for four minutes (Oren et al., 2018). Two percent agarose gels were loaded with 10uL of DNA and 1 uL of dye.

DNA Extracted from an Axenic *G. morbida* Culture and *P. juglandis* Beetle Tissues Serial Dilutions for PCR Limits

To better understand the limits of the current PCR protocol process, fungal and vector DNA from axenic *G. morbida* cultures (DNA type 1, Table 2.1) or whole beetle *P. juglandis* samples (DNA type 2, Table 2.1) at varying concentrations were tested to determine the lower detectable limits that can be achieved using the optimized protocol. For the serial dilutions, the concentrations of *G. morbida* and *P. juglandis* DNA were determined using a Nanodrop Spectrophotometer. Four different *G. morbida* samples were diluted with 0.1 TAE buffer (Tris

base, acetic acid, and ethylenediaminetetraacetic acid) at 12 concentrations ranging from 3.0 ng/µL to 0.00125 ng/µL concentrations. Four *P. juglandis* DNA samples were diluted to 11 concentrations ranging from 0.75 ng/µL to 0.0006 ng/µL. These samples were used to test the lowest detection rate on a conventional gel and QIAxcel Advanced capillary electrophoresis system. The last concentration resulting in a Relative Fluorescent Unit (RFU) reading about 0.05 RFUs was considered the lower limit for that sample with that primer set.

Serial Dilutions of Drilled Bark Shaving Samples

Serial dilutions were performed with the drilled bark shaving DNA (DNA types 3 and 4, Table 2.1). The drilled bark shaving DNA dilutions were not put to identical DNA concentrations before trials. Instead, the samples were diluted serially in one-to-one step-wise concentrations from the original recommended volume of one microliter. Subsequent dilution volumes were each reduced by half until the QIAxcel Advanced capillary electrophoresis system RFU reading was below 0.05 RFUs and the conventional gel no longer had a positive band. In this way, the first dilution contained 50% of the starting concentration, the second contained 25% of original, the third contained 12.5%, and so forth. Four *G. morbida* (GS004) positive drilled bark shaving samples (DNA type 3, Table 2.1) from *J. hindsii* trees in California, four *G. morbida* (GS004) positive drilled bark shaving samples from *J. nigra* trees in Tennessee, and four *P. juglandis* (WTB009) positive drilled bark shaving samples (DNA type 4, Table 2.1) from California were tested at concentrations ranging between 100% and 0.8% of recommended 1.0 ul concentrations.

Bark Sample Constructs Dilutions

A bark sample construct (DNA types 5 and 6, Table 2.1) was created using *G. morbida* and *P. juglandis*-negative samples from the Oren et al. (2018) Missouri branch drilling. Added to these extractions were *G. morbida* or *P. juglandis* DNA at varying concentrations by volume. This procedure was intended to replicate a field-collected sample, like a *G. morbida* or *P. juglandis* DNA-positive drilled bark shaving sample, but that contained a known starting concentration of each of the target species and *J. nigra* DNA. Due to low sample volumes available from DNA extractions recovered by Oren et al. (2018) from individual drill shaving samples, the volumes of multiple negative individual drilling samples were pooled from branch drillings that were taken from an individual tree. By pooling these 10 individual samples into a single, tree-based sample, a sufficient total volume of extracted DNA was available for use in assessing the detection capability of *G. morbida* and *P. juglandis* DNA within bark sample construct across a dilution-by-sample experiment. Each bark sample construct had a final *J. nigra* DNA concentration of 7 ng/µL. This concentration was comparable to the final DNA concentration found in Oren et al.'s (2018) drilled bark shaving samples and tested by Oren et al. and earlier in this study (about 7-10 ng/µL per sample, data not shown). The added *G. morbida* and *P. juglandis* DNA concentrations were at concentrations between 0.15 ng/µL and 0.0005 ng/µL. These concentrations were chosen based on the *G. morbida* and *P. juglandis* DNA serial dilution thresholds. This experiment was designed to determine if the presence of host-plant *J. nigra* DNA has any effect on the lower threshold of the QIAxcel Advanced capillary electrophoresis system or conventional gel systems. Four bark sample constructs containing *G. morbida* (DNA type 5, Table 2.1) and four bark sample constructs containing *P. juglandis* (DNA type 6, Table 2.1) were created and tested for this assay.

Copy Number Calculations

In species for which the full genome size is known, the nanogram concentration of DNA in a sample can be used to calculate an equivalent copy number obtained by DNA amplification for that species (Staroscik, 2004). This calculation can be performed for *G. morbida* samples because the genome size *G. morbida* has been determined (Schuelke et al., 2016), but not for *P. juglandis* samples because the genome for this species has not been published. A simplified equation (Fig. 2.1) is used to derive the copy number contained within the sample on the basis of input variables including the known length in base pair of the *G. morbida* genome (26.5 Mb), the weight of a nucleotide base pair, and the starting concentration of DNA (Schuelke et al., 2016). Each copy of a genome will equal one cellular-equivalent for *G. morbida*; therefore, by calculating the copy number within the diluted sample, an estimate can be made of how many cellular-equivalents of *G. morbida* are present within each µL of that sample before PCR is performed.

2.4 Results

Serial Dilution of Samples containing *G. morbida* and *P. juglandis* DNA

A conventional gel could replace the QIAxcel Advanced capillary electrophoresis system for positive identification in the case of DNA extracted from an axenic *G. morbida* cultures (DNA type 1, Table 2.1) and *P. juglandis* beetle tissues (DNA type 2, Table 2.1). Four *G. morbida* samples (DNA type 1, Table 2.1) were diluted to 12 different concentrations through serial dilutions (Table 2.1). A threshold of 0.05 relative fluorescent units (RFUs) was used to determine if a sample yielded a positive or negative test result. Of the concentrations tested with the four samples, the lowest sample concentration that met the RFU threshold contained 0.00125

ng/µL *G. morbida* DNA. The conventional gel lower detection limit was 0.0025 ng/µL. Four vector-derived *P. juglandis* samples (DNA type 2, Table 2.1) were also diluted to 11 different DNA concentrations in serial dilutions (Table 2.1). The QIAxcel Advanced capillary electrophoresis system and conventional gel both could detect *P. juglandis* in diluted samples down to 0.00125 ng/µL.

For comparison, the Oren et al. 2018 protocol used 1 uL of undiluted DNA whose concentration was not determined. Upon testing the concentrations of those samples for this study, the concentrations fell between 3 and 10 ng/µL per sample tested (data not shown).

Serial Dilutions of Drilled Bark Shaving Samples

Similar to *G. morbida* and *P. juglandis* DNA, a positive test result could be achieved with presence of much less drilled bark shaving DNA (DNA types 3 and 4, Table 2.1) than was originally used at 1uL of DNA per sample in the earlier Oren et al. (2018) protocol. Four samples of DNA that were extracted from infested *J. hindsii* tree branch sections collected in California had previously yielded positive detection results for *G. morbida* DNA (DNA type 3, Table 2.1) (Oren et al. 2018). For this study, these same samples examined again, after serially diluting nine times by volume instead of concentration (Table 2.2). Volume was used instead of concentration because the sample was comprised of a mix of *J. hindsii* and *G. morbida* DNA and contained unknown concentrations of each. The QIAxcel Advanced capillary electrophoresis system was able to detect *G. morbida* DNA presence in diluted samples that contained as little as 6% of the used 1µL volume as indicated by the Oren et al. (2018) protocol. The conventional gel was also able to detect DNA concentrations at 1.6% of the recommended 1µL volume. This sampling procedure was repeated with serial dilutions to five concentrations using four *J. nigra* tree samples from Tennessee that had also tested positive for *G. morbida* (DNA type 3, Table

2.1) (Oren et al., 2018). QIAxcel Advanced capillary electrophoresis system and conventional gel were both able to detect *G. morbida* DNA with 6% of the used 1µL volume (Table 2.3). Four drilled bark shaving samples from California that had previously tested positive for presence of *P. juglandis* DNA (DNA type 4, Table 2.1) were diluted to eight different concentrations (Table 2.3). The QIAxcel Advanced capillary electrophoresis system and conventional gel were able to detect *P. juglandis* DNA concentrations that were just 3% of the previously used volume.

Bark Sample Construct Dilution Tests

Bark sample constructs (DNA types 5 and 6, Table 2.1) were used to assay whether or not the presence of *J. nigra* or *J. hindsii* DNA within a bark sample construct would have an effect on the detection rate of the optimized protocol. Four drilled, bark shaving samples comprised of *G. morbida* (DNA type 5, Table 2.1) and *J. nigra* (DNA type 6, Table 2.1) DNA were tested at eight fungal DNA concentrations ranging between 0.15 ng/µL and 0.001 ng/µL (Table 2.3). The detection limit on the QIAxcel Advanced capillary electrophoresis system and conventional gel was 0.001 ng/µL of fungal DNA (DNA type 5, Table 2.1). Four bark sample constructs comprised of *P. juglandis* plus *J. nigra* DNA (DNA type 6, Table 2.1) were also tested across nine different dilution concentrations (Table 2.4). The detection limit on the QIAxcel Advanced capillary electrophoresis system was a beetle DNA (DNA type 6, Table 2.1) concentration 0.0005 ng/µL, while the conventional gel detection limit was 0.001 ng/µL.

2.5 Conclusions

Findings from this study confirm that the QIAxcel Advanced capillary electrophoresis system may be replaced with a conventional gel system while still yielding robust detection of target species DNA in drill shaving samples. This modification will significantly reduce the cost of equipment required to assay for presence of *G. morbida* and *P. juglandis* DNA within a

submitted suspect sample. A QIAxcel Advanced capillary electrophoresis system costs tens of thousands of dollars (US) in 2019, whereas a conventional gel system costs under $3,000. Many diagnostic labs with limited budgets are unable to purchase QIAxcel Advanced capillary electrophoresis system may already have the equipment needed to assay using conventional gels.

Results of this study show that the amount of drilled bark shaving sample DNA required to yield a positive test result is extremely low. Although, diluting will not be necessary for diagnostic purposes, it is likely that DNA will be diluted as a consequence of taking multiple drill shaving collections to obtain a complex sample from the branch of a TCD-suspect tree (WEK, personal communications). Based on copy number, only around four cellular equivalents per µl need be obtained to confirm presence of *G. morbida* or *P. juglandis* DNA in a sample.

The protocol is extremely sensitive to detect *G. morbida* or *P. juglandis* DNA even in the presence of non-target *J. nigra* DNA. The bark sample construct detection was comparable to the fungal culture derived and vector derived samples, and in some cases yielded lower limits than *G. morbida* or *P. juglandis* DNA alone. The observation that the lower limit thresholds from different sample types presents a challenge regarding potential for introducing mechanical error at extremely low concentrations of fungal or beetle vector DNA within a sample. More testing is needed to quantify the limits of dilutions by grouping samples; however, we expect this method to not be a practical limitation for the protocol.

3 A Novel Molecular Toolkit for Rapid Thousand Cankers Disease Diagnosis using Molecular Probes

3.1 Abstract

This report demonstrates an improved molecular methodology for diagnosing the presence of a causal plant pathogen or a primary insect vector, by means of visualizing a positive test result that indicates presence of a conserved region of the target species' DNA. The model experimental system includes diagnosis of a fungal plant pathogen, *Geosmithia morbida*, and a primary vector bark beetle, *Pityophthorus juglandis*, which together cause thousand cankers disease (TCD) in susceptible host plants that include *Juglans* (walnuts/butternuts) and *Pterocarya* (wingnut) species. Although there is an existing molecular protocol that can be used to assay for presence of the pathogen and vector DNA, the available protocol requires expensive equipment and technical expertise of end-users. For faster adoption by diagnostic laboratories, the existing protocol must be made easier to visualize, thus requiring readily available or easily obtainable lab equipment. Findings presented here document an improved method for enhanced identification step by replacing expensive equipment and providing simplified, quicker protocol for TCD detection. Here, we reduce the post-PCR identification to a simple blue light visualization test. Under a specific wavelength (440-460 nm), suspect test sample returns a positive result by emitting green fluorescence, while negative test results emit a red fluorescence. This protocol is sensitive to the presence of very small amounts of target species' DNA within a sample. Testing has also indicated experimental specificity that restricts possibility of false positive detections. Cross-transferability is limited in amplification success to the presence of non-target fungi or beetle species DNA. This novel protocol has ease of use that can be directly applied and quickly adopted by regulatory agents and diagnosticians throughout the range of thousand cankers disease.

3.2 Introduction

Thousand cankers disease (TCD) is an emerging plant disease complex between walnut and butternut (*Juglans* spp.) and wingnut species (*Pterocarya* spp.), the bark beetle *Pityophthorus juglandis*, and the fungal pathogen *Geosmithia morbida* (Tisserat et al., 2009; Kolařík et al., 2011; Seybold et al., 2013b; Hishinuma et al., 2016). While many tree species can be affected by TCD, *Juglans nigra* is the most susceptible species in the current range of the pathogen in the United States, whereas European native *J. regia* is under threat in Italy (Tisserat et al., 2009; Montecchio et al., 2015; Seybold et al., 2019). As adult and larval beetles tunnel through the phloem and cambium of the tree, beetles can introduce and distribute necrotic canker-causing *G. morbida* conidia and hyphae (Newton and Fowler, 2009; Seybold et al., 2013b). The galleries of the beetles and cankers of the pathogen girdle the tree, causing wilting, yellowing leaves, and premature dieback (Tisserat et al., 2009; Seybold et al., 2013b). In *J. nigra*, this TCD damage progresses across three to four years and can eventually cause tree death; however, in some areas, such as the southeast, tree decline can be slower (Kolařík et al., 2011; Seybold et al., 2019).

TCD damage is often mistaken for drought damage while nearly all visible signs pointing to the actual cause lies hidden beneath the bark (Daniels et al., 2016). To identify the pathogen, a small branch section can be collected and the upper layers of bark removed, enabling sampling from suspect lesions and cankers (Oren et al., 2018). To ensure that the signs or symptoms observed are caused by *G. morbida*, the sample of the lesion has be excised from the branch and cultured in a lab for two to six weeks. Utilizing a molecular approach, the same outcome can be achieved by using drilled bark shaving samples of phloem and some wood tissues and screening it for *G. morbida* or *P. juglandis* using species-specific microsatellite loci (Hadziabdic et al.,

2012; Hadziabdic et al., 2015; Oren et al., 2018). The molecular test involves collecting a sample of potentially infested wood, extracting DNA, and running PCR to determine if the sample is positive for *G. morbida* or *P. juglandis* (Oren et al., 2018). While this technique can be completed within a day, the current protocol requires specialized, expensive equipment, technical training, and sampling expertise. There is a critical need to make this protocol more user-friendly and reduce the equipment and labor costs involved. Molecular probes, such as molecular beacons and TaqMan probes, are oligonucleotide-based tools made to fluoresce under certain conditions that can be used to meet that goal.

Molecular beacons are oligonucleotides, or short DNA sequences with modifications, that can be used as probes to help identify the presence of a specific target DNA sequence (Tyagi and Kramer, 1996). These probes have a stem-and-loop structure that consists of a single-stranded DNA sequence plus a fluorescent "reporter" molecule on one side, and a quencher or "silencer" sequence on the other side (Fig. 3.1). The loop's DNA sequence is designed to be specific to a complimentary target sequence found within the target organism's DNA. When the loop structure finds its complementary DNA sequence within a "positive" test sample, the beacon will anneal to and hybridize with the target DNA (Fig. 3.1). This annealing separates the fluorescent molecule and quencher, causing fluorescence. This fluorescence continues until a denaturation step or polymerase knocks the beacon off its complementary sequence (Tyagi and Kramer, 1996).

As an alternative to molecular beacons, TaqMan probes are oligonucleotide probes that are designed to identify a specific DNA sequences amplified during PCR (Holland et al., 1991). The probes are comprised of three of the same components that comprise a molecular beacon: a complementary DNA sequence, a reporter, and a silencer (Fig. 3.1). Unlike molecular beacons,

TaqMan probes do not have a stem and loop structure. Also, unlike the molecular beacons, TaqMan probes are hydrolyzed into small fragments during the extension step of PCR by the TaqMan protocol-specific polymerase (Fig. 3.2). This allows for the permanent physical separation of the reporter and silencer. TaqMan fluorescence remains active permanently, as the reporter and silencer remain apart.

Detection of results from the molecular beacon and TaqMan probes are quantified by using the fluorescence resonance energy transfer (FRET) produced by the probe under controlled conditions. These probes have been designed for use within a qPCR machine, which for this study is a QuantStudio 6 Flex Real-Time PCR System (Applied Biosystems, Foster City, CA, USA). The qPCR machine measures the level of fluorescence emitted by molecular probes or dyes that become bound to target DNA sequences provided by a primer during amplification. With each cycle, the DNA template is amplified and the fluorescence signal increases. The signal increases because there are more copies of the complementary DNA present as the PCR runs. This specialized machine measures the difference in fluorescence across time and among samples. While molecular beacons and TaqMan probes are designed for use in a qPCR machine, a few studies have noted that the fluorescence of molecular beacons can be viewed outside of a qPCR thermocycler (Kostrikis et al., 1998; Qian et al., 2018). Our study is based on the concept that positive test results with fluorescent probes can be visualized independently from use with a qPCR machine.

The goals of this study are to take the current molecular method of TCD diagnosis and develop a novel molecular toolkit for rapid visual diagnosis that can be achieved using an efficient and reliable molecular probe. Achieving this objective would allow the current

molecular method of TCD diagnosis to be used without a QIAxcel Advanced capillary electrophoresis system, and instead a simple blue light visualization test.

3.3 Materials and Methods

DNA Extractions from Cultures of Known Fungal Species and *P. juglandis* Habitat-Associated Beetle Species

Samples of DNA from *G. morbida* axenic cultures and *P. juglandis* were isolated using the QIAamp Fast DNA Stool Mini Kit (Qiagen, Germantown, MD, USA) per the manufacturer's protocol. The calculated concentration of DNA, in nanograms per microliter (ng/µl), were recorded using a NanoDrop Microvolume Spectrophotometer (ThermoFisher, Waltham, MA, USA).

Drilled Bark Shaving Samples Extractions

An output from the Oren et al. (2018) study included 1600 drill shaving samples taken from *J. nigra* branches that were then assayed using microsatellite locus GS004. These individual samples were available for use in this project. For original sample collections, bark was removed from *J. nigra* branch sections using a sterilized scalpel to reveal cankers. Cankers and lesion margins were then drilled with a drill bit put through a modified microfunnel, where the bottom 1.5 mm was cut from microcentrifuge tube, on the cankers. The drilled shavings of phloem and some wood tissues were transferred into a 1.5 microcentrifuge tube. The tools were sterilized between samples and these tubes were kept frozen at -20ºC until processing. DNA was isolated from the drilled bark shaving samples using the QIAamp Fast DNA Stool Mini Kit (Qiagen, Germantown, MD, USA) per the manufacturer's protocol. These samples represent the

actual field-collected specimens from TCD-suspect trees that form an example of a real-world application that this protocol will enable.

Molecular Beacon and TaqMan Probe Design

To optimize future detection of *G. morbida* or *P. juglandis* DNA from samples suspected to be infested, molecular beacon and TaqMan probes were designed to target previously established microsatellite locations within the *G. morbida* and *P. juglandis* genomes. For this study the GS004 (*G. morbida* specific) and WTB09 (*P. juglandis* specific) microsatellite loci were used (Hadziabdic et al., 2012; Hadziabdic et al., 2015). These established primers were utilized for designing molecular beacons using the program Beacon Designer 8 (Premier Biosoft, Palo Alto, CA), while the TaqMan probes were designed in the PrimerQuest design program (IDT, Coralville, Iowa). Both molecular beacon and TaqMan probes were ordered from IDT with the 5' fluorophore FAM attached as the reporter and 3' Iowa Black® fluorescence quencher.

Molecular Beacon qPCR Protocol

Molecular beacon qPCR reactions contained 2 µL DNA, 8 µL Go-Taq G2 Hot Start Colorless Master Mix (Promega, Madison, WI, USA), 2 µL of each primer, 1 µL dimethyl sulfoxide (DMSO), 3 µL of sterile water, and 2 µL of molecular beacon probe for a total volume of 20 µL. Each run included a positive control of beetle-derived or fungal-derived DNA and a negative control of sterile water. qPCR was run in QuantStudio 6 Flex Real-Time PCR System in 96-well plates. The thermocycler was set to an initial denaturation step of 3 minutes at 94ºC, then 35 cycles of 94ºC for 40 seconds, 60ºC for 40 seconds, and 72ºC for 30 seconds, followed by a final extension of 72ºC for four minutes. The machine measured fluorescence during the 72ºC extension step when the probe is attached.

TaqMan Probe qPCR Protocol

Taqman qPCR reactions contained 10 µL of TaqMan Fast Advanced Master Mix, 2 µL of each primer, 2 µL of TaqMan probe, 2 µL of DNA, and 2 µL of water for a total reaction volume of 20 uL. Each run included a positive control of beetle-derived or fungal-derived DNA and a negative control of master mix and sterile water. qPCR was run in the in QuantStudio 6 Flex Real-Time PCR System at: 50ºC for two minutes, 95ºC for twenty seconds, then twenty cycles of denaturation at 95ºC for three seconds and annealing/extension at 60ºC for thirty seconds, followed by twenty cycles of denaturation at 95ºC for three seconds and annealing/extension at 55ºC for thirty seconds. Fluorescence was measured during the 60/55ºC annealing/extension steps.

Fluorescence Visualization

Probe fluorescence was quantified using a QuantStudio 6 Flex Real-Time PCR System and results were visualized using a NightSea Dual Fluorescent Protein Flashlight (NightSea, Lexington, MA, USA). Fluorescence is visualized by introducing external blue light of a specific excitation wavelength (440-460 nm), after which, the fluorescent molecule emits a lower, specific wavelength (Fig. 3.3). This new emission wavelength can be visualized by placing a filter in front of the users' eyes or a camera. The filter blocks out the excitation wavelength, leaving only the emission to be visualized. For this project the fluorophores used were FAM, which has an excitation of 495 nm and an emission of 520 nm, and ROX, which has an excitation wavelength of 575 nm and an emission wavelength of 602 nm. In this application, FAM is used to assay a sample for presence of a specific section of target DNA, while ROX is used as a fluorescing, passive reference dye. The NightSea flashlight that projects a narrow beam light across a 440-460 nm spectrum and is used with special glasses that filter out the 440-460

nm blue light wavelength. Although the spectrum of wavelengths generated by this blue light source is not perfectly aligned to the optimal wavelength for FAM and ROX, the unit still allows for visualization of FAM and ROX.

Molecular Beacon and TaqMan Probe Testing

To test the practicality of these probes, each was screened using with *G. morbida* DNA (DNA type 1, Table 2.1), GS004 microsatellite primer, and amplicon-specific fluorescing probes. The same test was replicated with *P. juglandis* DNA (DNA type 2, Table 2.1), WTB09 microsatellite primer and amplicon-specific fluorescing probes. These positive test samples were compared against a DNA-negative, sterile water sample. All samples were tested twice to provide a technical replication for each. The probes were tested in a QuantStudio 6 Flex Real-Time PCR System. Next, the fluorescence was visualized using the NightSea flashlight and filtering glass system. Once a working protocol was established, the protocol was tested in a SimpliAmp™ Thermal Cycler (Applied Biosystems, Foster City, CA, USA) followed by a visualization step using the NightSea light source to determine if positive test results enabled by the toolkit could be visualized independent of need for the QuantStudio 6 Flex Real-Time PCR System.

TaqMan probe qPCR with Drilled Bark Shaving Samples

In order to demonstrate that this novel protocol assayed for fungal or beetle DNA in drilled bark shaving samples, 20 samples (10 from Tennessee, 10 from California) that were positive for *G. morbida* (DNA type 3, Table 2.1) and 9 samples (from California) that were positive for *P. juglandis* (DNA type 4, Table 2.1) from the Oren et al. (2018) study were tested in

with the new protocol in the QuantStudio 6 Flex Real-Time PCR System, and visualized with the NightSea light source. This experiment shows the practical use of this new toolkit.

Serial dilutions of DNA extracted from an axenic *G. morbida* culture and *P. juglandis* beetle tissues for qPCR limits

After creating a working PCR protocol with the TaqMan probes, the protocol was tested with serially diluted starting concentrations of target-species DNA (DNA types 1 and 2, Table 2.1). This assay allowed for a better understanding of detection limits using the qPCR reaction. Dilutions were achieved using one-to-one serial dilutions from a known starting concentration of DNA extracted from either *G. morbida* fungal cultures (DNA type 1, Table 2.1) or *P. juglandis* beetle tissues (DNA type 2, Table 2.1). The concentrations of beetle-derived and fungal-derived DNA were determined with a Nanodrop Spectrophotometer. These dilutions were tested with a single sample in two technical replications that had been previously found positive on a conventional gel and in the QIAxcel Advanced capillary electrophoresis system. Dilutions from the sample were run in duplicates at 14 different DNA concentrations from 3.0 ng/µL to 0.00125 ng/µL. The samples were diluted in 0.1 TE buffer at a 1:1 dilution until DNA in samples was no longer detectable (a negative response). This result meant that amplifications failed to advance sample detection at levels higher than the set threshold in the QuantStudio 6 Flex Real-Time PCR System. A negative response also meant that the samples appeared red using the blue light visualization system.

Bark Sample Construct Dilution Tests

Bark sample constructs (DNA types 5 and 6, Table 2.1) were performed by taking negative drilled bark shaving samples and adding a known concentration of *G. morbida* or *P. juglandis* DNA (DNA types 5 and 6, Table 2.1). These samples each contained a final drilled

bark shaving sample DNA concentration of about 7 ng/µL, which is comparable to the concentrations of drilled bark shaving sample DNA (about 7-10 ng/µL)(data not shown). The *G. morbida* DNA or *P. juglandis* DNA (DNA types 5 and 6, Table 2.1) amount was decreased by half from sample to sample until the lower threshold is for a positive result was found. This gave an estimate of how much target DNA is needed in a drilled, bark shaving sample for the test to exhibit positive results. This test had three *G. morbida* bark sample constructs (DNA type 5, Table 2.1) run at six concentrations that ranged from 0.6 and 0.008. *P. juglandis* bark sample constructs (DNA type 6, Table 2.1) run at nine different concentrations that ranged between 0.15 ng/µL and 0.0005 ng/µL.

Cross-Transferability studies for TaqMan Probes

In order to ensure that the new GS004 and WTB09 TaqMan probes amplify only target species' DNA, the toolkit was tested against other fungal and beetle species. For *G. morbida*, this included 19 samples of various species of fungi, as well as five *Geosmithia* species, including *G. morbida,* tested in qPCR. These fungi samples were used in Oren et al. (2018) for cross-amplification and primer specificity. After that test 19 other samples of various species were also tested using qPCR. Then, 20 different beetle species DNA were tested in qPCR against the WTB09 primers and probe. These were the same bark beetle samples used in the Emel et al. (2018) study.

3.4 Results

Molecular Beacon Probe Testing

A molecular beacon probe was designed to supplement the previously published GS004 primer set (Hadziabdic et al., 2012). This beacon was tested with the same thermocycler protocol published for conventional PCR at first; however, products achieved using this protocol were of

limited quantity and quality (Oren et al., 2018). It was hypothesized that the probes may need higher annealing temperatures. Two polymerase master mixes were screened—Go-Taq G2 Hot Start Colorless Master Mix and Amplitaq Gold Master Mix. Both master mixes worked with the primers annealing at 60ºC. Next, PCR was performed under the Oren et al. published conditions (2018), but modified to use the 60ºC annealing temperature. Both master mixes amplified in qPCR, but the Amplitaq polymerase provided less background fluorescence and higher above-threshold results, so was better suited for qPCR and therefore used for further experiments.

Once functional probes were achieved using the thermocycler, molecular beacon visualization was assessed using the NightSea flashlight (Table 3.7). Validation of this latter step addresses a principle goal of the experiment, because simply changing from a QIAxcel Advanced capillary electrophoresis system to a qPCR machine would not substantively reduce the costs of purchase and maintenance of requisite equipment. For molecular beacons, the background fluorescence was too high to enable use of the probes outside of a qPCR machine. While the qPCR did confirm that negative and positive samples would appear slightly different in color, both were visible in shades of green using the NightSea flashlight (Fig. 3.5). To restrict confounding influences of the future protocol, and to make results easier to interpret, a negative test result using a molecular beacon probe would need to be clear, not green. To further assess the scope of the problem, a tube of pre-PCR master mix (alone) was tested under the blue wavelength light and this sample also appeared green. This suggests that the silencer and reporter are too close together on the probe (Fig. 3.5) to prevent fluorescence. Additional study of the structure of the probe would be needed to confirm that theory. These troubleshooting steps are beyond the scope of this study, so efforts were re-focused on use of the TaqMan probes.

TaqMan Probe Testing

TaqMan probes were designed for use with the GS004 and WTB09 previously published primer sets. Recommended thermocycler settings from the TaqMan Fast Advanced Master Mix were used, with one alteration. Based on the molecular beacon information we wanted to include 60ºC annealing, then go down to 55ºC as a touchdown PCR protocol. Given the restrictions of the qPCR machine, this was not possible, so instead, 20 cycles with a 60ºC annealing temperature and 20 cycles with a 55ºC annealing temperature were used. This method functioned well and we used this procedure for the remainder of our tests (Table 3.9).

Next, the Taqman probes were visualized outside the qPCR machine with the NightSea handheld blue light source. The TaqMan Fast Advanced Master Mix does include a passive reference dye, ROX, which allows the qPCR machine to measure results and compare values to emissions from the fluorescent probe. This ROX reference dye is visible at the same wavelength used to visualize FAM fluorescence, thus providing a test result whereby negative samples appear red and positive samples appear green (Table 3.10). If samples are visualized prior to running PCR, the pre-PCR sample solution will be visible as emitting fluorescence in a red hue (Table 3.10).

TaqMan Probe qPCR with Drilled Bark Shaving Sample DNA

The GS004 TaqMan probe was tested against 20 known *G. morbida* positive samples from Oren et al. (2018) (DNA type 3, Table 2.1); 10 from Tennessee and 10 from California-sourced *J. nigra* branch samples. These samples all tested positive for presence of *G. morbida* DNA, both with the optimized qPCR protocol, and were visibly green using the blue light source visualization screening.

The same procedures were repeated with the WTB09 probe and nine drill shaving samples (DNA type 4, Table 2.1) that were from California-sourced *J. nigra* branches, which had also tested positive for *P. juglandis* DNA using QIAxcel Advanced capillary electrophoresis system (Oren et al. 2018). All but one of these samples tested negative on both the qPCR machine and under the blue light visualization screening.

Fungal Culture Derived and Beetle Derived DNA Serial Dilutions for qPCR Limits

Serial dilutions of fungal culture-derived DNA were performed to determine the lowest concentrations of *G. morbida* that the qPCR and blue light visualization protocols could detect a positive test result. The GS004 probe was tested in one sample (DNA type 1, Table 2.1) consisting of two technical replications across 14 decreasing DNA concentrations (Table 3.1), which ranged from 14.0 ng/µL to 0.0008 ng/µL. The qPCR threshold was found to be 0.003 ng/µL, and the visual blue light threshold was 0.025 ng/µL. The WTB09 probe was also tested with one sample (DNA type 2, Table 2.1) consisting of two technical replications. There were 10 decreasing concentrations (Table 3.1) that ranged from 0.75 ng/µL to 0.0006 ng/µL. The qPCR threshold was 0.005ng/µL and the visual blue light threshold was 0.009 ng/µL. At DNA concentrations lower than 0.009 ng, sample appearance in tubes became mottled leading to end-user difficulty in visually deciphering a positive from a negative test result (Fig. 3.8).

Bark Sample Constructs Dilutions

qPCR was performed using the GS04 probes against bark sample constructs DNA (DNA types 5 and 6, Table 2.1) to test the sensitivity of the qPCR and blue light visualization protocols. Three samples (DNA type 5, Table 2.1), with two technical replications, were tested at six concentrations of *G. morbida* DNA that ranged from 0.6 to 0.008 ng/µL (Table 3.2). The lowest qPCR threshold was 0.02 ng/µL and the blue light visualization threshold was 0.04 ng/µL.

The WTB09 probes were also used with bark sample constructs (DNA type 6, Table 2.1) to determine the lower threshold of the qPCR and blue light visualization protocols. Three samples (DNA type 6, Table 2.1) with two technical replications were tested across nine decreasing DNA concentrations (Table 3.2), which ranged from 0.15 ng/µL to 0.005 ng/µL beetle DNA. The lowest qPCR threshold was 0.02 ng/µL, and the blue light visualization threshold was 0.15 ng/µL.

Cross-Transferability studies for TaqMan Probes

The *G. morbida* TaqMan probe was tested for cross-transferability to different fungal species, using the 19 samples screened by Oren et al. (2018) (Table 3.3). In the Oren et al. study using the QIAxcel Advanced capillary electrophoresis system, none of these samples amplified. In qPCR, three fungal samples amplified similarly to *G. morbida*, the positive control. Seven other fungal species amplified above the threshold during the last three cycles of qPCR. Beyond the qPCR, these three samples that amplified comparable to *G. morbida* were also visible under the NightSea light source. The samples that crossed the threshold during the last three cycles were not visible under the handheld blue wavelength light. However, these samples used by Oren et al. (2018) were all taken from *J. nigra* and *J. hindsii* TCD infested trees. DNA obtained in these samples was obtained from fungal cultures that may have contained several *G. morbida* spores, not detectable by ITS1 and ITS 4 primers.

To further examine cross-transferability of the GS004 primers and the fluorescing probe, 19 samples from other plant sources were taken and tested for cross-amplification (Table 3.4). Six showed minor, late-cycles amplification (cycle 37-38), like the first assay with Oren et al. (2018) samples, but none amplified earlier. None of the samples except the positive control were visible under the NightSea light source. This secondary assay does not fully test the theory of *G.*

morbida contamination, because *Alternaria burnsii*, *Ophiostoma nigrocarpum,* and *O. narcissi* from plant sources different than *J. nigra* were not tested. However, other related species were tested, including *A. arborescens*, *A. alternata,* and *O. colliferium* were found to be negative. This supports the efficacy of microsatellite primers in that these primers do not cross-amplify between genera, and often not between different species within a genus.

The TaqMan probe designed with the WTB09 primer to screen for *P. juglandis* DNA was tested for cross-transferability in 20 beetle species that had been assayed in Oren et al. (2018) (Table 3.5). Many of these species are commonly active within the *J. nigra* crown and therefore must not cross-amplify for this protocol to be effective (Chahal, 2017; Klingeman et al., 2017). None yielded positive test results for either the qPCR or under the NightSea light, supporting observation that the protocol is very specific to *P. juglandis.*

3.5 Discussion and Conclusions

Molecular beacons did not work for our purposes. Although molecular beacons could be used in a qPCR setting, the background fluorescence was too high to use in a NightSea visualization setting. The beacons probes were designed to be extremely stringent for our target *G. morbida* and *P. juglandis* sequences, and theoretically that should have reduced the likelihood of nonspecific fluorescence (Goel et al., 2005; Hadziabdic et al., 2012; Hadziabdic et al., 2015). However, in practice, the nonspecific fluorescence was very high, even before PCR. This result could be explained by many different factors. More than likely, however, the beacon is not folded properly and so prevents fluorescence before PCR. Further studies with redesigned molecular beacon probes would be required to use this probe as we have intended.

TaqMan probes worked with both *G. morbida* (DNA type 1, Table 2.1) and *P. juglandis* DNA (DNA type 2, Table 2.1), as well as *G. morbida* and *P. juglandis* bark sample constructs

(DNA types 5 and 6, Table 2.1). *Geosmithia morbida* positive drilled bark shaving samples (DNA type 3, Table 2.1) were able to amplify in this system; however, further tests with new drilled bark shaving samples will be needed for more testing of the *P. juglandis* probe with the drilled bark shaving sample protocol (DNA type 4, Table 2.1). The observed negative response is likely because the positive reactions in the Oren et al. (2018) tests had these samples as very low DNA and very low RFU (0.1-0.05, data not shown) in testing with the QIAxcel Advanced capillary electrophoresis system. More than likely, these samples had extremely little *P. juglandis* DNA present for the qPCR to amplify. Consequently, the protocol may not be viable for drilled bark shaving samples if looking specifically for *P. juglandis*, yet is still functional for detecting *G. morbida* DNA. The test was readily adaptable for *G. morbida*-positive, drilled bark shaving samples (DNA type 3, Table 2.1). These tests also show the low amounts of DNA that are needed to produce a positive test result in a drill-shaving sample, particularly compared to the recommended concentrations in the Oren et al. (2018) protocol.

The TaqMan protocol provides a visual method for differentiating between a positive, or visible green, test result versus a negative, or visible red, test result. This protocol allows for immediate result identification without the need for a conventional gel or the QIAxcel Advanced capillary electrophoresis system. Adopting this protocol will make the tests easier to use and results more readily interpreted by the end users, especially when eliminating need for the qPCR machine. Importantly, qPCR positives closer to the threshold do not appear positive under the blue light visualization test, as the red and green color may be mottled. It may be advantageous to have the end user of this toolkit follow the heavily encouraged practice of including a negative and positive control in tests to compare the fluorescence and protect against false positives and/or negatives.

Cross-transferability results suggest that cultures that were believed to have been axenic, or cultures thought to be free of contamination, may have contained *G. morbida* hyphal cells or conidia within the sample that confounded expected test results. Future contamination can be mitigated by not using samples from *J. nigra* as negative controls, particularly if samples may be collected from a TCD-infested area. The positive result also highlights the sensitivity of this protocol to detect minute amounts of DNA. These confounding results could lead to false positive interpretations from qPCR. This problem can be avoided by eliminating the last three to five cycles of qPCR amplification which that appear to be replicating non-target DNA pieces. The removal of these last amplification cycles would not be necessary if using the NightSea visualization technique because none of the samples that were late cycle amplifications in qPCR appeared positive under the blue light (440-460 nm) visualization.

Cross-transferability of beetle DNA was found to be negative. This is particularly important because many of the tested beetle species are active throughout the *J. nigra* crown and a few of these species have been found to carry *G. morbida* (Chahal, 2017; Klingeman et al., 2017). While these beetles are not effective at spreading *G. morbida*, it encourages the use of both *P. juglandis* and *G. morbida* identification in thousand cankers disease recognition. The presence of the pathogen without the beetle has been found, but the damage is ineffective without both the pathogen and vector (Hadziabdic et al., 2014b; Chahal, 2017).

4 Conclusions

This research was able to replace the QIAxcel Advanced capillary electrophoresis system in the Oren et al. (2018) protocol with either a conventional gel or a blue light visualization test. Both the conventional gel and blue light visualization tests allow for a reduction in cost to begin using this protocol, as well as a reduction in cost per sample. These new protocols are easier to use than the QIAxcel Advanced system, particularly for the blue light protocol that only requires shining a blue wavelength light on the sample at the protocol step that previously required the QIAxcel Advanced capillary electrophoresis system.

The conventional gel and blue light visualization methods each have advantages and disadvantages. The conventional gel method takes one to two hours to complete, longer than the blue light visualization method, and user will need to make or order gels before the assay can be performed. However, the conventional gel is considerably more sensitive than the blue light visualization method. The conventional gel yields positive test results for bark sample constructs constructed using both *G. morbida* (DNA type 5, Table 2.1) and *P. juglandis* (DNA type 6, Table 2.1) samples with concentrations as low as 0.001 ng/µL. By contrast, the blue light visualization method detected positive results for the same bark sample constructs containing *G. morbida* and *P. juglandis* DNA, but only at concentrations as low as 0.04 ng/µL and 0.15 ng/µL, respectively. It is important to note that for *G. morbida*, drilled bark shaving samples tested positive with the blue light visualization test, however, success to detect *P. juglandis* DNA will require more testing, in part, due to the false negative test results that were observed using the light visualization procedure. While blue light visualization is less sensitive than conventional gels, the method is faster, cheaper, and easier. Once DNA has been amplified, samples can be

tested with cheaper equipment. Diagnosticians, who are tasked to screen for *G. morbida* and *P. juglandis* in suspect tree samples, could implement these new protocols almost immediately.

The costs of the starting equipment are notably different between the Oren et al. (2018) QIAxcel Advanced capillary electrophoresis system protocol and modifications reported here for conventional gel and blue light visualization methods. A principle difference is evident for startup costs associated with equipment. The QIAxcel Advanced capillary electrophoresis system and supporting software together cost tens of thousands of dollars. A conventional gel system, for example using an Invitrogen™ E-Gel™ Power Snap Electrophoresis System, costs about $3,000. Many labs may already have similar equipment. As another alternative, the blue light visualization protocol requires the purchase of a NightSea blue light at about $210 and blue light excluding glasses, at about $40. These changes in cost, from almost forty thousand dollars to about two hundred dollars, makes the new protocol much more accessible to smaller labs.

This study also uses the TaqMan probe technology in a novel way. To our knowledge this is the first study using TaqMan probes for rapid visual identification external to use with a qPCR system. While molecular beacons have been used in this way for similar study goals, the procedure and probe was not effective because of the high background fluorescence making it difficult to view the difference between samples testing positive and negative for target species DNA. This observation is contrary to other published descriptions of molecular beacon use, because typically the background fluorescence is very low (Marras et al., 2006). By contrast, TaqMan probes are often considered easier to design and less prone to structural issues, such as stem and loop interferences where extra stems are formed in the loop, when compared to molecular beacons (Kolpashchikov, 2012). TaqMan probes are also much cheaper to order for

testing (Kolpashchikov, 2012). We expect that this research will open possibilities within the field of molecular probes by allowing for cheaper testing than molecular beacons.

We plan to conduct several additional tests before presenting these new protocols to potential users. For example, we will be assessing new samples of drilled bark shaving samples to further examine the blue light visualization test with use in *P. juglandis*-positive samples. From results observed for bark sample constructs, the protocol is expected to consistently detect *G. morbida* DNA from drilled bark shaving samples taken from field-collected TCD suspect branch tissues. To date, however, the protocol has not performed as well with samples believed to contain *P. juglandis* DNA. The drilled bark shaving samples that were used presented very low RFUs on the QIAxcel Advanced capillary electrophoresis system used in the Oren el al. study (2018), so the blue light visualization may not be sensitive enough for detection of *P. juglandis.* More tests are needed to validate that hypothesis. Second, more cross-transferability screening will increase confidence in the validity of sample results. We plan to assess several different *Ophiostoma* spp. and *Alternaria* spp. with the *G. morbida*–specific probe. If axenic cultures can be obtained, future tests would ideally include *Alternaria burnsii, Ophiostoma nigrocarpum,* and *O. narcissi* from host sources that were not *J. nigra.*

Moving forward, there is still a great deal of research that can be done with these new protocols to decrease the protocol's cost, time, and effort requires. Despite the blue light visualization protocol ease of use, the conventional gel protocol could still be very useful if, when modified slightly, a sample could be multiplexed to simultaneously screen for presence of both *G. morbida* and *P. juglandis* DNA; positive detections of each within a sample would be visualized by presence of two specifically-sized bands in the gel matrix. This latter step would save end users both time and money. With adjustment, the blue light visualization protocol may

also be able to be modified for multiplexing. For example, removing the ROX from the current TaqMan probes system may allow for negative samples to appear clear instead of red, as was the expectation with molecular beacons. If the removal of ROX was successful, a CY5-based probe that provides a visible emission spectrum appearing red could be used for one target species, FAM (appearing green) for the other DNA of interest, with mottled colors indicating a positive test result for both *G. morbida* and *P. juglandis*, while a clear sample would indicate a negative test result for both species.

Beyond multiplexing, this protocol could be made simpler by moving towards an isothermal reaction. While a thermocycler is not a particularly expensive piece of equipment (as low as $400), adaptation of the protocol for an isothermal reaction could allow the protocol to be taken out of the lab and into a thermos in the field (Nkouawa et al., 2012). Achieving this step would require considerable changes to the protocol, but there are many examples of practicality for this use that makes optimizing for isothermal reactions especially promising (Notomi et al., 2000; Li et al., 2017; Shin et al., 2018).

If the purchase cost for the QIAxcel Advanced capillary electrophoresis system is excluded, the next largest cost that accrues per sample are consumable costs associated with the DNA extraction step. There are many methods for DNA extraction found throughout the literature that incur various costs. A good step moving forward for this protocol would be simplifying the DNA extraction step. This would save not only money but time, particularly if a direct PCR protocol could be used. The biggest impediment to that method is utility with different sample types. There have, however, been instances in which wood shavings have been used for direct PCR amplification (Niessen and Vogel, 2010; Sillo et al., 2018). Use of direct

PCR would save considerable time and costs of each sample, while making that step significantly easier for the end-user.

Finally, this protocol has been focused on yielding reliable screening evidence of presence of TCD complex member DNA, in part because this plant pathogen is difficult to recover from infected *J. nigra* collected in the eastern US, and because field diagnosis of TCD is challenging in the field because disease symptoms are readily confused with drought damage. Overlooking disease expression in the landscape can allow the disease to persist at low levels for years, thereby allowing additional spread of the disease. There are many other plant pathogens and insect pests that could be adapted for screening procedures using the knowledge gained in this study. For example, key pest insect DNA could be assayed from within a complex sample of insect species collected en masse to a general insect attractant lure (e.g., ethanol bait or other pheromone attractant). Pathogen species of interest could similarly be sampled following DNA extraction from a complex water sample taken from a nursery irrigation supply or groundwater (pond) source. Presence of beneficial plant endophytes (e.g., *Trichoderma* spp. and *Beauveria* spp.) could be screened from within surface-sterilized plant tissues.

References

Audley, J., Mayfield, A., Myers, S., Taylor, A., and Klingeman, W. (2016). Phytosanitation methods influence posttreatment colonization of *Juglans nigra* logs by *Pityophthorus juglandis* (Coleoptera: Curculionidae: Scolytinae). Journal of Economic Entomology *109*, 213-221.

Audley, J., Taylor, A., Klingeman, W.E., Mayfield, A.E., and Myers, S.W. (2015). Insecticide dip treatments to prevent walnut twig beetle colonization of black walnut logs. Forest Products Journal *60*, 233-240.

Barnes, B.V., and Spurr, S.H. (1998). Forest ecology, 4th edition. New York:New York, Wiley Publishing.

Bernard, A., Lheureux, F., and Dirlewanger, E. (2018). Walnut: past and future of genetic improvement. Tree Genetics & Genomes *14*, 1-28.

Blood, B.L., Klingeman, W.E., Paschen, M.A., Hadžiabdić, Đ., Couture, J.J., and Ginzel, M.D. (2018). Behavioral responses of *Pityophthorus juglandis* (Coleoptera: Curculionidae: Scolytinae) to volatiles of black walnut and *Geosmithia morbida* (Ascomycota: Hypocreales: Bionectriaceae), the causal agent of thousand cankers disease. Environmental Entomology, *47*(2):412-421. doi: 10.1093/ee/nvx194

Bright, D.E. (1981). Taxonomic monograph of the genus *Pityophthorus Eichhoff* in North and Central America (Coleoptera, Scolytidae). Memoirs of the Entomological Society of Canada *113*, 1-378.

Cawkwell, L., Bell, S., Lewis, F., Dixon, M., Taylor, G., and Quirke, P. (1993). Rapid detection of allele loss in colorectal tumours using microsatellites and fluorescent DNA technology. Br J Cancer *67*, 1262-1267.

Chahal, K., R. Gazis, W. Klingeman, D. Hadziabdic, P. Lambdin, J. Grant, and M. Windham (in preparation). Assessment of alternative candidate beetle vectors from walnut crowns in habitats quarantined for thousand cankers disease. Journal of Economic Entomology. (Accepted)

Chahal, K.S. (2017). Thousand Cankers Disease: Virulence of *Geosmithia morbida* isolates and potential alternative vectors of the fungus. In Entomology and Plant Pathology (University of Tennessee, Knoxville, TN University of Tennessee M.S. Thesis), 1-89.

Daniels, D., Nix, K., Wadl, P., Vito, L., Wiggins, G., Windham, M., Ownley, B., Lambdin, P., Grant, J., Merten, P., *et al.* (2016). Thousand cankers disease complex: A forest health issue that threatens *Juglans* species across the U.S. Forests *7*, 260.

Fisher, J.R., McCann, D.P., and Taylor, N.J. (2013). *Geosmithia morbida*, thousand cankers disease of black walnut pathogen, was found for the first time in southwestern Ohio. Plant Health Progress doi:10.1094/PHP-2013-1201-01-BR.

Freeland, E. (2012). Intraspecific variability of *Geosmithia morbida* the causal agent of thousand cankers disease, and effects of temperature, isolate and host family (*Juglans nigra*) on canker development. In Department of Bioagricultural Sciences and Pest Management (Fort Collins, Colorado: Colorado State University, M.S Thesis).

Freeland, E., Cranshaw, W., and Tisserat, N. (2012). Effect of *Geosmithia morbida* isolate and temperature on canker development in black walnut. Plant Health Progress doi:10.1094/PHP-2012-0618-01-RS.

Gazis, R., Poplawski, L., Klingeman, W., Boggess, S., Trigiano, R., Graves, A., Seybold, S., and Hadziabdic, D. (2018). Mycobiota associated with insect galleries in walnut with thousand cankers disease reveals a potential natural enemy against *Geosmithia morbida*. Fungal Biology *122*, 241-253.

Ginzel, M., and Juzwik, J. (2014). *Geosmithia morbida*, the causal agent of thousand cankers disease, found in Indiana. HN-89-W West Lafayette, IN: Purdue Extension, Department of Entomology 2 p, 1-2.

Goel, G., Kumar, A., Puniya, A.K., Chen, W., and Singh, K. (2005). Molecular beacon: a multitask probe (Oxford, UK), pp. 435-442.

Goodell, E. (1984). Walnuts for the northeast. Arnoldia *44*, 2-19.

Grant, J.F., Windham, M.T., Haun, W.G., Wiggins, G.J., and Lambdin, P.L. (2011). Initial assessment of thousand cankers disease on black walnut, *Juglans nigra*, in eastern Tennessee. Forests *2*, 741-748.

Graves, A.D., Coleman, T.W., Flint, M.L., and Seybold, S.J. (2009). Walnut twig beetle and thousand cankers disease: Field identification guide. UC-IPM Website Publication, 2 pp.

Hadziabdic, D., Vito, L.M., Windham, M.T., Pscheidt, J.W., Trigiano, R.N., and Kolarik, M. (2014a). Genetic differentiation and spatial structure of *Geosmithia morbida*, the causal agent of thousand cankers disease in black walnut *(Juglans nigra*). Current Genetics *60*, 75-87.

Hadziabdic, D., Wadl, P., Staton, M., Klingeman, W., Moulton, J., Pscheidt, J., Wiggins, G., Grant, J., Lambdin, P., Windham, M., *et al.* (2015). Development of microsatellite loci in *Pityophthorus juglandis*, a vector of thousand cankers disease in *Juglans* spp. Conservation Genetics Resources *7*, 431-433.

Hadziabdic, D., Wadl, P.A., Vito, L.M., Boggess, S.L., Scheffler, B.E., Windham, M.T., and Trigiano, R.N. (2012). Development and characterization of sixteen microsatellite loci for *Geosmithia morbida*, the causal agent of thousand canker disease in black walnut (*Juglans nigra*). Conservation Genetics Resources *4*, 287-289.

Hadziabdic, D., Windham, M., Baird, R., Vito, L., Cheng, Q., Grant, J., Lambdin, P., Wiggins, G., Windham, A., and Merten, P. (2014b). First report of *Geosmithia morbida* in North Carolina: The pathogen involved in thousand cankers disease of black walnut. Plant Disease *98*, 992.

Hamelin, R.C., Bourassa, M., Jimmy, R., Dusabenyagasani, M., Jacobi, V., and Laflamme, G. (2000). PCR detection of *Gremmeniella abietina*, the causal agent of Scleroderris canker of pine. Mycological Research *104*, 527-532.

Hansen, M., Bush, E., Day, E., Griffin, G., and Dart, N. (2011). Walnut thousand cankers disease alert. In Virginia Cooperative Extension, 1-4.

Haun, G., Powell, S., Strohmeier, C., and Kirksey, J. (2010). State of Tennessee thousand cankers disease action plan. In Tennesseee Department of Agriculture, 1-34.

Hefty, A.R. (2016). Risk of invasion by walnut twig beetle throughout eastern North America Retrieved from the University of Minnesota Digital Conservancy, http://hdl.handle.net/11299/182824.

Hefty, A.R., Coggeshall, M.V., Aukema, B.H., Venette, R.C., and Seybold, S.J. (2016). Reproduction of walnut twig beetle in black walnut and butternut. HortTechnology *26*, 727-734.

Hishinuma, S.M., Dallara, P.L., Yaghmour, M.A., Zerillo, M.M., Parker, C.M., Roubtsova, T.V., Nguyen, T.L., Tisserat, N.A., Bostock, R.M., and Flint, M.L. (2016). Wingnut (*Juglandaceae*) as a new generic host for *Pityophthorus juglandis* (Coleoptera: Curculionidae) and the thousand cankers disease pathogen, *Geosmithia morbida* (Ascomycota: Hypocreales). The Canadian Entomologist *148*, 83-91.

Holland, P.M., Abramson, R.D., Watson, R., and Gelfand, D.H. (1991). Detection of specific polymerase chain reaction product by utilizing the 5' → 3' exonuclease activity of *Thermus aquaticus* DNA polymerase. Proceedings of the National Academy of Sciences of the United States of America *88*, 7276-7280.

Juzwik, O., McDermott-Kubeczko, M., Stewart, T., and Ginzel, M.D. (2016). First report of *Geosmithia morbida* on ambrosia beetles emerged from thousand cankers-diseased *Juglans nigra* in Ohio. Plant Disease *100*, 1238-1238.

Klingeman, W.E., Oliver, J.B., Bray, A.M., Ranger, C.M., and Palmquist, D.E. (2017). Trap style, bait, and height deployments in black walnut tree canopies help inform monitoring strategies for bark and ambrosia beetles (Coleoptera: Curculionidae: Scolytinae). Environmental Entomology *46*, 1120-1129.

Kolařík, M., Freeland, E., Utley, C., and Tisserat, N. (2011). *Geosmithia morbida* sp. nov., a new phytopathogenic species living in symbiosis with the walnut twig beetle (*Pityophthorus juglandis*) on *Juglans* in USA. Mycologia *103*, 325-332.

Kolařík, M., Kubatova, A., Hulcr, J., and Pazoutova, S. (2008). *Geosmithia* fungi are highly diverse and consistent bark beetle associates: evidence from their community structure in temperate Europe. Microbial Ecology *55*, 65-80.

Kolpashchikov, D.M. (2012). An elegant biosensor molecular beacon probe: Challenges and recent solutions. Scientifica *2012*, 928783, 1-17. http://dx.doi.org/10.6064/2012/928783

Kostrikis, L.G., Tyagi, S., Mhlanga, M.M., Ho, D.D., and Kramer, F.R. (1998). Spectral genotyping of human alleles. Science *279*, 1228-1229.

Lamarche, J., Potvin, A., Pelletier, G., Stewart, D., Feau, N., Alayon, D.I.O., Dale, A.L., Coelho, A., Uzunovic, A., Bilodeau, G.J., *et al.* (2015). Molecular detection of 10 of the most unwanted alien forest pathogens in Canada using real-time PCR. PloS One *10*, e0134265.

Lauritzen, J.E. (2018). Characterization of black walnut genotypes for resistance to thousand cankers disease, frost hardiness and other desirable horticultural traits. In Biology (Logan, UT: Utah State University), 1-46.

Lench, N.J., Norris, A., Bailey, A., Booth, A., and Markham, A.F. (1996). Vectorette PCR isolation of microsatellite repeat sequences using anchored dinucleotide repeat primers. Nucleic Acids Research *24*, 2190-2191.

Leslie, C.A., Seybold, S.J., Graves, A.D., Cranshaw, W., and Tisserat, N. (2010). Potential impacts of thousand cankers disease on commercial walnut production and walnut germplasm conservation. Acta Horticulturae *861*, 431-434.

Li, Y., Fan, P., Zhou, S., and Zhang, L. (2017). Loop-mediated isothermal amplification (LAMP): A novel rapid detection platform for pathogens. Microbial Pathogenesis *107*, 54-61.

Marras, S.A.E., Tyagi, S., and Kramer, F.R. (2006). Real-time assays with molecular beacons and other fluorescent nucleic acid hybridization probes. Clinica Chimica Acta *363* (1-2):48-60.

maryland.gov (2018). Walnut twig beetle and thousand cankers disease. Maryland Department of Agriculture. https://mda.maryland.gov/plants-pests/Pages/tcd.aspx. Accessed 15 April 2019.

Mayfield, A., Fraedrich, S., Taylor, A., Merten, P., and Myers, S. (2014). Efficacy of heat treatment for the thousand cankers disease vector and pathogen in small black walnut logs. Journal of Economic Entomology *107*, 174-184.

Mayfield, I.I.I.A.E., Audley, J., Camp, R., Mudder, B.T., and Taylor, A. (2018). Bark colonization of kiln-dried wood by the walnut twig beetle: Effect of wood location and pheromone presence. Journal of Economic Entomology, 1-4. https://doi.org/10.1093/jee/toy023

McDermott-Kubeczko, M. (2016). Fungi isolated from black walnut branches in Indiana and Tennessee urban areas. Retrieved from the University of Minnesota Digital Conservancy, https://conservancy.umn.edu/handle/11299/180201.

Montecchio, L., and Faccoli, M. (2014). First record of thousand cankers disease *Geosmithia morbida* and walnut twig beetle *Pityophthorus juglandis* on *Juglans nigra* in Europe. Plant Disease *98*, 696.

Montecchio, L., Fanchin, G., Simonato, M., and Faccoli, M. (2015). First record of thousand cankers disease fungal pathogen *Geosmithia morbida* and walnut twig beetle P*ityophthorus juglandis* on *Juglans regia* in Europe. Plant Disease *99*, 1183-1183.

Montecchio, L., Vettorazzo, M., and Faccoli, M. (2016). Thousand cankers disease in Europe: an overview. EPPO Bulletin *46*, 335-340.

Moricca, S., Bracalini, M., Benigno, A., Ginetti, B., Pelleri, F., and Panzavolta, T. (2018). Thousand cankers disease caused by *Geosmithia morbida* and its insect vector *Pityophthorus juglandis* first reported on *Juglans nigra* in Tuscany, Central Italy, Plant Disease, *103*(2), p. 369

Newton, L., and Fowler, G. (2009). Pathway Assessment - *Geosmithia* sp. and *Pityophthorus juglandis* Blackman movement from the western into the eastern United States. United States Department of Agriculture Animal and Plant Health Inspection Service, 1-50.

Nguyen, T.L. (2015). Studies of *Geosmithia morbida*, the causal agent of thousand cankers disease, and nonpathogenic *Geosmithia* species carried by *Pityophthorus juglandis* and their interaction with *Juglans* species of economic and ecological importance in California. In Plant Pathology (Davis, CA: University of California), 1-2.

Niessen, L., and Vogel, R.F. (2010). Detection of *Fusarium graminearum* DNA using a loop-mediated isothermal amplification (LAMP) assay. International Journal of Food Microbiology *140*, 183-191.

Nix, K.A. (2013). The life history and control of *Pityophthorus juglandis* Blackman on *Juglans nigra* L. in eastern Tennessee. In Entomology and Plant Pathology (Knoxville, TN: University of Tennessee M.S. Thesis), 1-93.

Nkouawa, A., Sako, Y., Li, T., Chen, X., Nakao, M., Yanagida, T., Okamoto, M., Giraudoux, P., Raoul, F., Nakaya, K., *et al.* (2012). A loop-mediated isothermal amplification method for a differential identification of *Taenia* tapeworms from human: Application to a field survey. Parasitology International *61*, 723-725.

Notomi, T., Okayama, H., Masubuchi, H., Yonekawa, T., Watanabe, K., Amino, N., and Hase, T. (2000). Loop-mediated isothermal amplification of DNA. Nucleic Acids Research *28*, e63-e63.

Oren, E., Klingeman, W., Gazis, R., Moulton, J., Lambdin, P., Coggeshall, M., Hulcr, J., Seybold, S.J., and Hadziabdic, D. (2018). A novel molecular toolkit for rapid detection of the pathogen and primary vector of thousand cankers disease. PloS One *13*, e0185087.

Paul, M., Jerome, G., Carla, C., Katheryne, N., and Paris, L. (2013). Concentration levels of imidacloprid and dinotefuran in five tissue types of black walnut, *Juglans nigra*. Forests *4*, 887-897.

Qian, C., Wang, R., Wu, C., Wang, L., Ye, Z., Wu, J., and Ji, F. (2018). A fast and visual method for duplex shrimp pathogens detection with high specificity using rapid PCR and molecular beacon. Analytica Chimica Acta *1040*, 105-111.

Randolph, K.C., Rose, A.K., Oswalt, C.M., and Brown, M.J. (2013). Status of black walnut (*Juglans nigra* L.) in the eastern United States in light of the discovery of thousand cankers disease. Castanea *78*, 2-14.

Rugman-Jones, P.F., Seybold, S.J., Graves, A.D., and Stouthamer, R. (2015). Phylogeography of the walnut twig beetle, *Pityophthorus juglandis*, the vector of thousand cankers disease in North American walnut trees. PloS One *10*, e0118264.

Saiki, R.K., Gelfand, D.H., Stoffel, S., Scharf, S.J., Higuchi, R., Horn, G.T., Mullis, K.B., and Erlich, H.A. (1988). Primer-directed enzymatic amplification of DNA with a thermostable DNA polymerase. Science *239*, 487-491.

Schlötterer, C., and Tautz, D. (1992). Slippage synthesis of simple sequence DNA. Nucleic Acids Research *20*, 211.

Schuelke, T.A., Westbrook, A., Broders, K., Woeste, K., and MacManes, M.D. (2016). De novo genome assembly of *Geosmithia morbida*, the causal agent of thousand cankers disease. PeerJ *4*, e1952.

Schuelke, T.A., Wu, G., Westbrook, A., Woeste, K., Plachetzki, D.C., Broders, K., and Macmanes, M.D. (2017). Comparative genomics of pathogenic and nonpathogenic beetle-vectored fungi in the genus *Geosmithia*. Genome Biology and Evolution *9*, 3312.

Serdani, M., Vlach, J., Wallis, K., Zerillo, M., McCleary, T., and N., T. (2013). First report of *Geosmithia morbida* and *Pityophthorus juglandis* causing thousand cankers disease in butternut. Plant Health Progress doi:10.1094/PHP-2013-1018-01-BR.

Seybold, S., Haugen, D., O'Brien, J., and Graves, A. (2013a). Thousand cankers disease. In USDA Forest Service, Northeastern Area State and Private Forestry Pest Alert NA-PR-02-10, 1-2.

Seybold, S.J., Coleman, T.W., Dallara, P.L., Dart, N.L., Graves, A.D., Pederson, L.A., and Spichiger, S.-E. (2012). Recent collecting reveals new state records and geographic extremes in the distribution of the walnut twig beetle, *Pityophthorus juglandis* Blackman (Coleoptera: Scolytidae), in the United States. The Pan-Pacific entomologist *88*, 277-280.

Seybold, S.J., Dallara, P.L., Hishinuma, S.M., and Flint, M.L. (2013b). Detecting and identifying the walnut twig beetle: Monitoring guidelines for the invasive vector of thousand cankers disease of walnut. (Oakland, California: University of California Agriculture and Natural Resources, Statewide Integrated Pest Management Program). www.ipm.ucdavis.edu/thousandcankers

Seybold, S.J., Klingeman, W.E., III, Hishinuma, S.M., Graves, A.D., and Coleman, T.W. (2019). Status and Impact of Walnut Twig Beetle in Urban Forest, Orchard, and Native Forest Ecosystems. Journal of Forestry *117*, 152-163.

Seybold, S.J., Penrose, R.L., and Graves, A.D. (2016). Invasive Bark and Ambrosia Beetles in California Mediterranean Forest Ecosystems. In Insects and Diseases of Mediterranean Forest Systems, T.D. Paine, and R. Lieutier, eds. (Cham, Switzerland: Springer International Publishing), 583-662.

Shin, D.-S., Heo, G.-I., Son, S.-H., Oh, C.-S., Lee, Y.-K., and Cha, J.-S. (2018). Development of an improved loop-mediated isothermal amplification assay for on-site diagnosis of fire blight in apple and pear. The Plant Pathology Journal *34*, 191-198.

Sillo, F., Giordano, L., and Gonthier, P. (2018). Fast and specific detection of the invasive forest pathogen *Heterobasidion irregulare* through a Loop- mediated isothermal AMPlification (LAMP) assay. Forest Pathology, *48*, e12396.

Silva, C.F.d., Uesugi, C.H., Blum, L.E.B., Marques, A.S.d.A., and Ferreira, M.Á.d.S.V. (2016). Molecular detection of *Erwinia psidii* in guava plants under greenhouse and field conditions. Ciência Rural *46*, 1528-1534.

Smejkal, G.B., and Lazarev, A. (2006). Separation methods in proteomics. Boca Raton: FL, CRC Taylor & Francis.

Staroscik, A. (2004). Calculator for determining the number of copies of a template. URI Genomics & Sequencing Center. https://cels.uri.edu/gsc/cndna.html. Accessed 11 April 2019.

Stone, D.E., Oh, S.-H., Tripp, E.A., and Manos, P.S. (2009). Natural history, distribution, phylogenetic relationships, and conservation of Central American black walnuts (*Juglans* sect. *Rhysocaryon*). The Journal of the Torrey Botanical Society *136*, 1-25.

Thousandcankers.com (2017). Distribution of thousand cankers disease as of August 1, 2017. http://thousandcankers.com/general-information/ Accessed 11 April 2019.

Tisserat, N., Cranshaw, W., Leatherman, D., Utley, C., and Alexander, K. (2009). Black walnut mortality in Colorado caused by the walnut twig beetle and thousand cankers disease. Plant Health Progress https://doi.org/10.1094/PHP-2009-0811-01-RS

Tisserat, N., Cranshaw, W., Putnam, M.L., Pscheidt, J., Leslie, C.A., Murray, M., Hoffman, J., Barkley, Y., Alexander, K., and Seybold, S.J. (2011). Thousand cankers disease is widespread in black walnut in the western United States. Plant Health Progress doi:10.1094/PHP-2011-0630-01-BR.

TN.gov, Tennessee Department of Agricultire (2018). Tennessee thousand canker disease quarantine map. https://www.tn.gov/content/dam/tn/agriculture/images/ThousandCankersMap.jpg. Accessed 11 April 2019.

Tsui, C.K.M., Roe, A.D., El- Kassaby, Y.A., Rice, A.V., Alamouti, S.M., Sperling, F.A.H., Cooke, J.E.K., Bohlmann, J., and Hamelin, R.C. (2012). Population structure and migration pattern of a conifer pathogen, *Grosmannia clavigera*, as influenced by its symbiont, the mountain pine beetle. Molecular Ecology *21*, 71-86.

Tyagi, S., and Kramer, F.R. (1996). Molecular beacons: probes that fluoresce upon hybridization. Nature Biotechnology *14*, 303-308.

USDA-FS-PPQ (2018). Thousand cankers disease survey guidelines for 2018. https://www.aphis.usda.gov/plant_health/plant_pest_info/tcd/downloads/TCD_Survey_Guidelines.pdf. Accessed 11 April 2019.

USDA (2013). Pest alert: Thousand canker disease. USDA Forest Service Northeastern Area State and Private Forestry. https://www.fs.usda.gov/naspf/sites/default/files/thousand_cankers_disease_print_res.pdf. Accessed 11 April 2019.

Utley, C., Nguyen, T., Roubtsova, T., Coggeshall, M., Ford, T.M., Grauke, L.J., Graves, A.D., Leslie, C.A., McKenna, J., Woeste, K., et al. (2013). Susceptibility of walnut and hickory species to *Geosmithia morbida*. Plant Disease *97*, 601-607.

Versalovic, J., and Lupski, J.R. (2002). Molecular detection and genotyping of pathogens: more accurate and rapid answers. Trends in Microbiology *10*, s15-s21.

Voulgaridis, V., and Vassiliou, V.G. (2005). The walnut wood and its utilisation to high value products. Acta Horticulturae, 69-81.

Whitehorn, P.R., O'Connor, S., Wackers, F.L., and Goulson, D. (2012). Neonicotinoid pesticide reduces bumble bee colony growth and queen production. Science *336*, 351.

Williams, R. (1990). Black walnut (*Juglans nigra* L.), Volume 2. Washington, DC, USDA.

Wood, S.L. (1982). The bark and ambrosia beetles of North and Central America (Coleoptera: Scolytidae), a taxonomic monograph. Great Basin Naturalist Memoirs *6*, 1-1359.

Zane, L., Bargelloni, L., and Patarnello, T. (2002). Strategies for microsatellite isolation: A review (Oxford, UK), pp. 1-16.

Zerillo, M., Ibarra Caballero, J., Woeste, K., Graves, A., Hartel, C., Pscheidt, J., Tonos, J., Broders, K., Cranshaw, W., Seybold, S., *et al.* (2014). Population structure of *Geosmithia morbida*, the causal agent of thousand cankers disease of walnut trees in the United States. PloS One *9*, e112847.

Appendix

Figures

$$number\ of\ copies\ = \frac{Conc.\times\ 6.022x10^{23}}{BP\ \times\ 1x10^{9}\ \times\ 650}$$

$$G.morbida\ number\ of\ copies\ = \frac{Conc.\times\ 6.022x10^{23}}{26500000\times\ 1x10^{9}\ \times\ 650}$$

Figure 2.1 Equation used for calculating *Geosmithia morbida* copy numbers. This figure shows how to calculate the copy number of a given sample. "Conc." equals the concentration of the DNA in ng/µL and "BP" equals the genome size in base pairs. *Geosmithia morbida* has a genome length of 26.5 Mb. That will be in input to "BP." The dilution concentration would be "Conc." This allows one to know about how many cellular units are in each dilution sample.

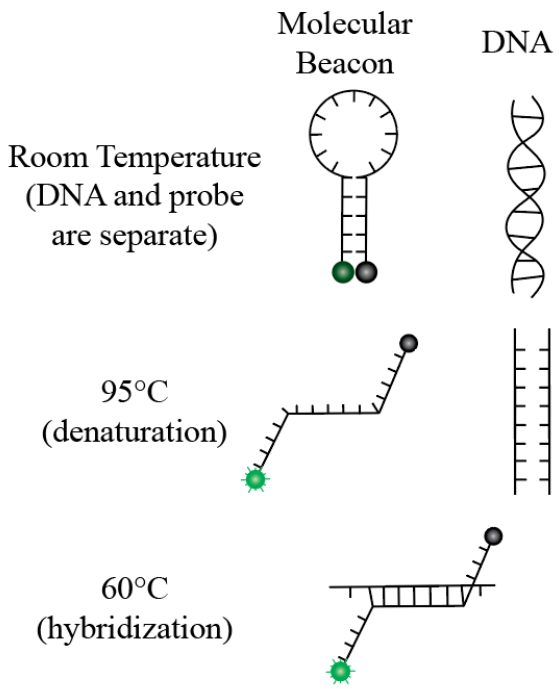

Figure 3.1 Molecular beacon structure and hybridization. Molecular beacons are short single-stranded DNA sequences that form a stem-and-loop structure. These probes are designed to identify the presence of a specific DNA sequence. The loop portion is comprised of a sequence complementary to a specific target sequence; in this case a flanking region of species-specific microsatellite loci. The stem portion is comprised of two complementary sequences that will hybridize with one another through presence of a fluorescent "reporter" fluorophore (green sphere) and a quencher or "silencer" (black sphere) on the other side. Without the target, the probe has no fluorescence because the reporter and silencer are in such proximity to one another. In the presence of the target DNA sequence, the beacon hybridizes with the sequence. This condition separates the fluorophore and quencher, resulting in fluorescence.

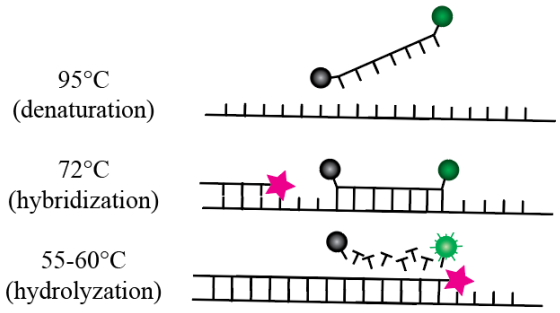

Figure 3.2 TaqMan probe structure, hybridization, and hydrolyzation. TaqMan probes are short single-stranded DNA sequences that do not form a secondary structure. The probe is comprised of the sequence complementary to a specific DNA sequence, a reporting fluorophore (green sphere), and a silencing quencher (black sphere). During PCR double stranded DNA is separated during the denaturation step. The TaqMan probes can attach during the hybridization step. During extension the probes are hydrolyzed by the polymerase (pink star), permanently removing the fluorophore from the quencher, allowing for fluorescence emission.

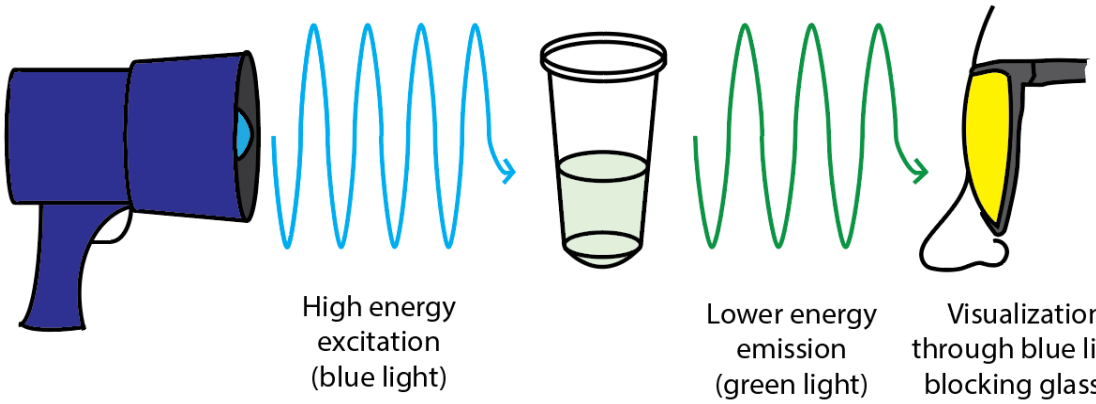

Figure 3.3 Fluorescence excitation and emission. Fluorescence becomes visually apparent when an external light of a specific wavelength (440-460 nm; excitation) is introduced to an oligonucleotide probe such as a TaqMan or molecular beacon probe that has been designed to fluoresce under specific conditions; in this case the presence of a target DNA sequence. When the fluorophore compound is excited, the probe emits a lower specific wavelength (525; emission). The new light is visualized by placing a filter in front of the eyes (blue light blocking glasses) that blocks out the excitation wavelength, allowing the user to easily see the emission.

A. 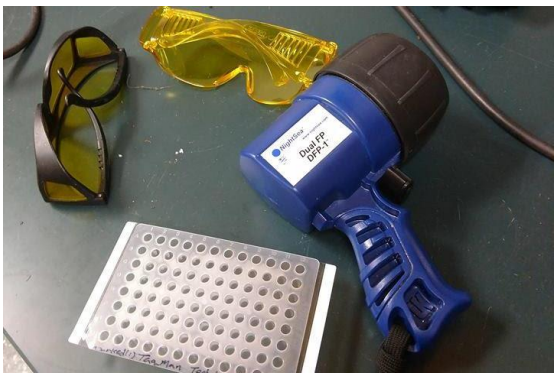

B. 

Figure 3.4 Fluorescence visualization with blue NightSea flashlight setup. The NightSea Dual Fluorescent Protein Flashlight, light specific glasses (filter), and a typical 96-well plate containing a qPCR reaction (A.). Results can be visualized with the NightSea light that reveals fluorescence when turned on and placed with the light pointing skyward. In practice, the 96-well plate is placed on top of the flashlight, with the glasses (filter) placed in front of the viewers' eyes or camera (B.). The glasses filter out light within the 460-480 nm wavelength, removing the blue light from the viewer's sight. This leaves only the emission of 520 nm for visualization. Because of the beam's narrow angle, only two samples at a time can be visualized using this setup.

A. 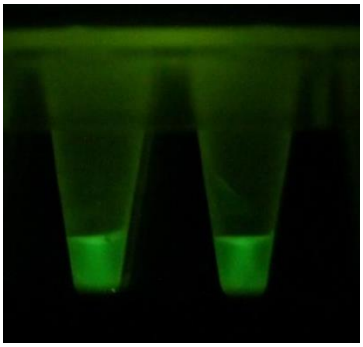 B. 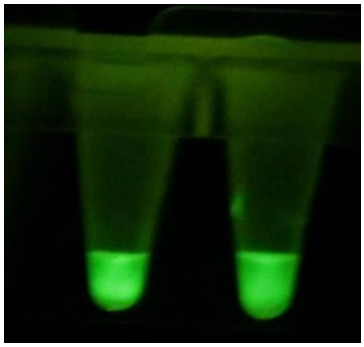 C. 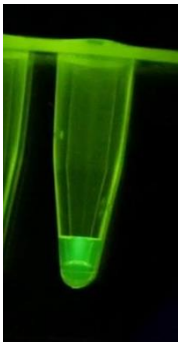

Figure 3.5 Molecular beacon visual results with *Geosmithia morbida* DNA. The leftmost image (A.) shows two negative samples and the center image shows two positive samples (B.) using the molecular beacon protocol. While a difference in intensity is apparent between A. and B., having presence of any fluorescence in the negative control limits accuracy for interpreting test results. The image to the right (C.) similarly shows the confounding appearance of a tube of molecular beacon even before PCR has been performed.

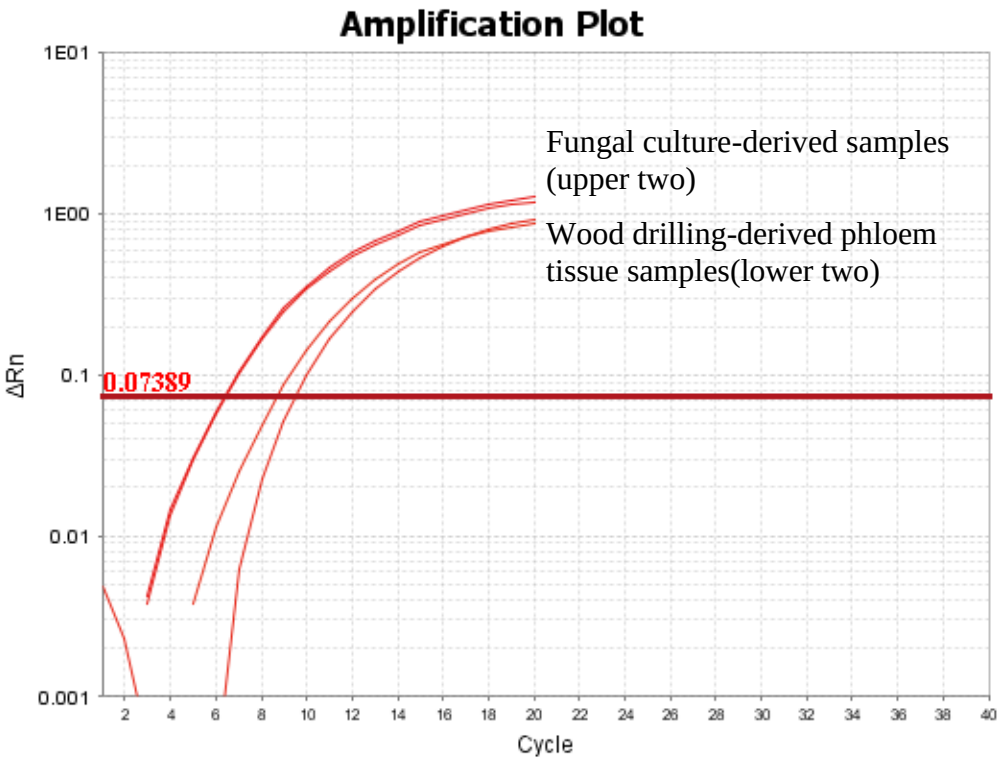

Figure 3.6 *Geosmithia morbida* TaqMan probe qPCR results. Results TaqMan probes trials in the QuantStudio 6 Flex Real-Time PCR System. DNA amplified in both the culture-derived fungal samples (A.) and wood drilling-derived phloem samples (B.), while the negative controls (water and master mix) did not amplify, therefore are not visible on this graph. Image from QuantStudio software results.

A. 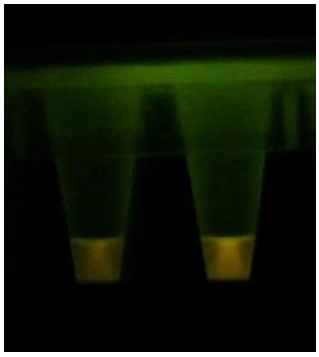 B. 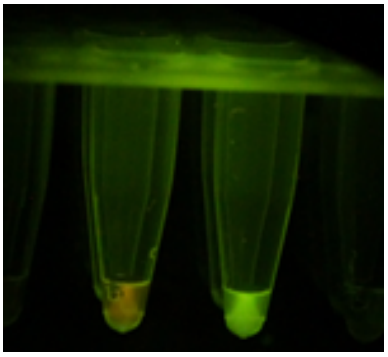

Figure 3.7 Visualization of test results using *Geosmithia morbida* primers and TaqMan probe. The image on the left (A.) has a negative water control in the first tube and a positive fungal sample in the second tube *before* PCR. The image on the right (B.) shows the same two samples after PCR has been performed. The negative remains a red color, attributed to presence of ROX in the solution, while a sample positive for detection of *G. morbida* DNA becomes green.

A. 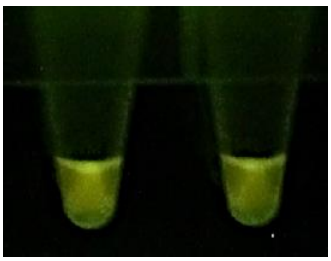 B. 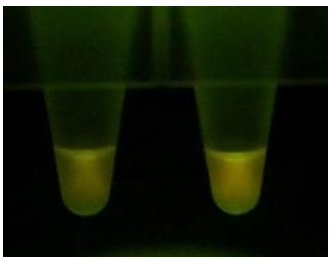

Figure 3.8 TaqMan culture-derived *Geosmithia morbida* DNA dilutions: visualization of highly diluted samples containing *Geosmithia morbida* DNA. The image on the left (A.) shows fluorescence in vials containing 0.025 ng *G. morbida* DNA per sample (by volume) in the PCR reaction. The image on the right (B.) has samples with 0.0125 ng *G. morbida* DNA per sample in the PCR reaction. The left image is clearly green, but the right image seems mixed and would be unclear based on the fluorescence alone.

Tables

Table 2.1 Various sample types names and descriptions. This table gives descriptions of each sample type used in chapters two and three.

Sample Type Number	Sample Name	Sample Description
Type 1	*Geosmithia morbida* DNA	Axenic culture derived *Geosmithia morbida* DNA
Type 2	*Pityophthorus juglandis* DNA	Whole beetle derived *Pityophthorus juglandis* DNA
Type 3	*Geosmithia morbida* drilled bark shaving sample	Drilled bark shaving sample from Oren et al. (2018) study that was found to be positive for *Geosmithia morbida*
Type 4	*Pityophthorus juglandis* drilled bark shaving sample	Drilled bark shaving sample from Oren et al. (2018) study that was found to be positive for *Pityophthorus juglandis*
Type 5	*Geosmithia morbida* bark sample construct	Drilled bark shaving sample from Oren et al. (2018) study from Missouri that was found to be negative for *Geosmithia morbida* plus the addition of axenic culture derived *G, morbida* DNA
Type 6	*Pityophthorus juglandis* bark sample construct	Drilled bark shaving sample from Oren et al. (2018) study from Missouri that was found to be negative for *Pityophthorus juglandis* plus the addition of whole beetle derived *P. juglandis* DNA

Table 2.2 Fungal culture derived *Geosmithia morbida* and vector derived *Pityophthorus juglandis* DNA dilution test results.

This table gives concentrations tested and results of the *G. morbida* and *P. juglandis* DNA dilution test.

Test	Concentrations tested (ng/µL) [A]	Sample ID [B]	QIAxcel minimum (ng/µL) [C]	Copy Number [D]	Conventional gel minimum (ng/µL) [E]	Copy number [D]
Culture derived *G. morbida* DNA dilutions	0.75, 0.56, 0.20, 0.11, 0.08, 0.06, 0.04, 0.02, 0.01, 0.005, 0.0025, 0.00125	GM27B	0.01	35	0.02	70
		GM33B1	0.08	280	0.04	140
		GM35	0.005	17.5	0.005	17.5
		GM47	0.00125	4.37	0.0025	8.74
Vector derived *P. juglandis* DNA dilutions	0.75, 0.37, 0.18, 0.09, 0.04, 0.02, 0.01, 0.005, 0.0025, 0.00125, 0.006	WTB9WA	0.0025	*N/A*	0.00125	*N/A*
		WTB10WA	0.0025	*N/A*	0.0025	*N/A*
		WTB11WA	0.0025	*N/A*	0.0025	*N/A*
		WTB21WA	0.01	*N/A*	0.0025	*N/A*

[A] Concentration values list all the concentrations tested for a given experiment.
[B] Sample code is the name given by Oren et al. (2018), for the sample evaluated in this study.
[C] QIAxcel Minimum reports the lowest concentration before the RFU fell below 0.05 ng/µl.
[D] Copy number is the number of cellular units per 1 µL for the given QIAxcel Advanced capillary electrophoresis system or conventional gel minimum concentration.
[E] The conventional gel minimum is the minimum concentration at which a gel produced a band.

Table 2.3 *Geosmithia morbida* and *Pityophthorus juglandis* drilled bark shaving sample dilution test results. This table gives the concentrations tests and results of the drilled bark shaving sample dilution tests.

Test	Concentrations tested [A] (uL, % by volume)	Sample code [B]	QIAxcel minimum [C]	Conventional gel minimum [D]
***G. morbida* positive wood drilling derived DNA (from CA) dilutions**	100%, 50%, 25%, 12.5%, 6.25%, 3%, 1.6%, 0.8%, 0.4%	CA5	6.25%	3%
		CA389	6.25%	1.6%
		CA280	6.25%	6.25%
		CA379	6.25%	3%
***G. morbida* positive wood drilling derived DNA (from TN) dilutions**	100%, 50%, 25%, 12.5%, 6.25%	TCD4	6.25%	6.25%
		TCD26	6.25%	6.25%
		TCD9	6.25%	6.25%
		12R2	6.25%	6.25%
***P. juglandis*-positive wood drilling derived DNA (from CA) dilutions**	100%, 50%, 25%, 12.5%, 6.25%, 3%, 1.6%, 0.8%	CA34	6.25%	1.6%
		CA224	6.25%	3%
		CA94	6.25%	3%
		CA167	*N/A*	*N/A*

[A] Concentration values list all the concentrations tested for a given experiment.
[B] Sample code is the name given by Oren et al. (2018), for the sample evaluated in this study.
[C] QIAxcel Minimum reports the lowest concentration before the RFU fell below 0.05 ng/µl.
[D] The conventional gel minimum is the minimum concentration at which a gel produced a band.

Table 2.4 QIAcel Advanced and convention gel bark sample construct dilution assay. Concentrations used in dilution series of *Juglans* spp. sampled branch *Geosmithia morbida* and *Pityophthorus juglandis* DNA from phloem and wood tissues of the archetypal drill shaving sample dilution tests as well as the concentrations tested.

Test name	Concentrations tested (ng/µL) [A]	Sample code [B]	QIAxcel minimum (ng/µL) [C]	Copy number [D]	Conventional gel minimum (ng/µL) [E]	Copy number [D]
***G. morbida* positive wood drilling derived mock-up sample dilutions**	0.15, 0.075, 0.037, 0.018, 0.009, 0.005, 0.002, 0.001	GM27B	0.001	3.5	0.001	7
		GM33B1	0.009	31.5	0.005	17.5
		GM35	0.001	7	0.001	7
		GM47	0.001	7	0.001	7
***P. juglandis* positive wood drilling derived mock-up sample dilutions**	0.15, 0.064, 0.032, 0.016, 0.008, 0.004, 0.002, 0.001, 0.0005	WTB9WA	0.0005	*N/A*	0.002	*N/A*
		WTB10WA	0.001	*N/A*	0.001	*N/A*
		WTB11WA	0.001	*N/A*	0.001	*N/A*
		WTB21WA	0.0005	*N/A*	0.004	*N/A*

[A] Concentration values list all the concentrations tested for a given experiment.
[B] Sample code is the name given by Oren et al. (2018), for the sample evaluated in this study
[C] QIAxcel Minimum reports the lowest concentration before the RFU fell below 0.05 ng/µl.
[D] Copy number is the number of cellular units per 1 uL for the given QIAxcel or conventional gel minimum concentration.
[E] The conventional gel minimum is the minimum concentration at which a gel produced a band.

Table 3.1 Serial dilution trials for detecting lower limits of qPCR detectability for *Geosmithia morbida* and *Pityophthorus juglandis* DNA. This table covers the fungal culture-derived and beetle-derived qPCR experimental results.

Probe-adapted primer	Concentrations tested (ng/µL) [A]	qPCR threshold [B]	Blue light threshold [C]
GS004	14.0, 3.5, 1.8, 0.9, 0.4, 0.2, 0.1, 0.05, 0.025, 0.013, 0.006, 0.003, 0.0016, 0.0008	0.003	0.025
WTB09	0.75, 0.37, 0.18, 0.09, 0.04, 0.02, 0.01, 0.005, 0.00125, 0.0006	0.005	0.09

[A] Concentration values list all the concentrations tested for a given experiment.
[B] qPCR threshold gives the lowest concentration before the amplification fell below the program given threshold.
[C] Blue light threshold gives the lowest concentration before the sample color under blue light was mottled, as defined as green and red mixed.

Table 3.2 qPCR and blue light visualization bark sample construct dilution assay. This table covers the fungal culture derived mock wood drilling samples and beetle derived mock wood drilling samples dilutions qPCR experimental results.

Probe	Dilutions (ng/µL) [A]	Sample code [B]	qPCR Threshold [C]	Light Threshold [D]
GS004	0.6, 0.15, 0.08, 0.04, 0.02, 0.008	GM27B	0.02	0.08
		GM33B1	0.02	0.6
		GM35	0.02	0.04
WTB09	0.15, 0.08, 0.04, 0.02, 0.008, 0.004, 0.002, 0.001, 0.005	WTB9WA	0.08	0.15
		WTB10WA	0.04	0.15
		WTB11WA	0.02	0.15

[A] Concentrations show all the concentrations tested for a given experiment.
[B] Sample code is the name given by Oren et al. (2018), for the sample evaluated in this study
[C] qPCR threshold gives the lowest concentration before the amplification fell below the program given threshold.
[D] Blue light threshold gives the lowest concentration before the sample color under blue light was mottled, as defined as green and red mixed.

Table 3.3 Non-*Geosmithia* based fungal DNA samples taken from *Juglans nigra* wood samples from Oren et al. (2018). These samples had all been tested previously using the QIAxcel Advanced capillary electrophoresis system protocol, with all being negative. However, when tested against the qPCR protocol, three samples came up positive and seven samples passed the threshold in the last two to three cycles (denoted with a asterisks). Table modified from Oren et al. (2018).

Strain[A]	Amplification with GS004	BLAST ID	GenBank Accession
NGM33-2	NO	*Chaetothyrium agathis* MFLUCC 12-0113	NR_132914
NGM33-9	NO	*Aureobasidium pullulans* strain CBS 584.75	KT693733
NGM33-11	NO	*Cladosporium pini-ponderosae* strain CBS 124456	NR_119730
NGM33-13	NO*	*Tremella aurantia* strain CBS 6965	AF444315
NGM33-16	NO*	*Alternaria destruens* ATCC 204363	NR_137143
NGM34-3	NO	*Ceratocystiopsis collifera (Ophiostoma colliferum)* CBS 126.89	NR_103597
NGM34-18	NO*	*Cladosporium pini-ponderosae* strain CBS 124456	NR_119730
NGM34-32	NO*	*Yamadazyma mexicana* CBS:7066	EF568069
NGM34-36	YES**	*Ophiostoma nigrocarpum* strain CMW1468	AF484457
NGM34-38	YES**	*Alternaria burnsii* CBS 107.38	NR_136119
NGM34-40	YES**	*Ophiostoma narcissi* strain CBS138.50	AY194510
NGM35-10	NO	*Diatrypella atlantica* voucher HUEFS 194228	KM396615
NGM35-12	NO*	*Pezicula sporulosa strain* CBS 225.96	KR859262
NGM35-21	NO*	*Alternaria alternata* strain ATCC 6663	KU729030
NGM35-22	NO	*Phaeoacremonium viticola* strain CBS 101738	KF764574
NGM36-12	NO	*Alternaria arborescens* strain MUCL 44260	DQ242505
NGM36-17	NO	*Cladosporium cladosporioides* strain ATCC 6721	KP780438
NGM36-19	NO*	*Pichia hampshirensis* strain ATCC 62896	FJ381694
NGM36-20	NO	*Epicoccum nigrum* strain UAMH 3247	AY625064

[A] Strain is the name given by Oren et al. (2018), for the sample evaluated in this study

** See discussion for more information.

Table 3.4 Cross-transferability test: Fungal samples not derived from *Juglans nigra*. Based on the results of Table 3.3, more testing of the GS004 probe was necessary. These samples were taken from any host plant source except *J. nigra*. While some crossed the qPCR threshold in the last three cycles (denoted with an asterisk), none were positive earlier in the amplification cycling and none were visible under the light visualization test.

Sample code[A]	Fungal species[B]	Positive on qPCR	Green under blue light
DH1	*Insolibasidium deformans*	No	No
CheatPM	*Blumeria graminis*	No	No
GreengoldPM2	*Golovinomyces spadiceus*	No*	No
Henbit PM2	*Neoerysiphe galeopsidis*	No	No
Epazote Downy	Epazote with Downy Mildew	No*	No
VP609B	*Erysiphe pulchra*	No	No
W94B	*Discula* spp.	No	No
PT14	*Peronospora tabacina*	No*	No
1/98	*Pseudoperonospora* spp.	No*	No
PC19	P. cubensis	No	No
R3	*Rhizoctonia* spp. on *Pityopsis*	No	No
C3	*Curvularia* spp. on *Pityopsis*	No	No
Tonula 25-1	*Tonula* spp.	No	No
soil 1	Unknown soil pathogens	No	No
soil2	Unknown soil pathogens	No	No
soil 3	Unknown soil pathogens	No	No
K	*Myrothecium* spp.	No*	No
Fus	*Fusarium* spp.	No*	No
PC	*Phytophthora capsici*	No	No
Pos. control	*G. morbida*	Yes	Yes
Neg. control	Sterile, DI water	No	No

[A] Strain is the name given by laboratory groups who gave these samples

[B] Sample description, including species name, if known

Table 3.5 Non-*Pityophthorus Juglandis* bark beetle derived DNA samples taken from *Juglans nigra* wood samples from Oren et al. (2018). These samples had all been tested previously using the QIAxcel Advanced capillary electrophoresis system protocol, with all being negative. When tested with the qPCR protocol none were positive except the positive control, *P. juglandis* sample. Table modified from Oren et al. (2018).

Beetle Species (Family: Subfamily)	(Collection location) County, State	Amplification of WTB09
Curculionidae: Cossinae		
Stenoscelis brevis	Anderson, TN	NO
Curculionidae: Cossoninae		
Stenomimus pallidus	Knox & Blount, TN	NO
Curculionidae: Scolytinae		
Cnestus mutilatus	Anderson & Knox, TN	NO
Euwallacea validus	Anderson, TN	NO
Hypothenemus crudiae	Knox, TN	NO
Monarthrum mali	Knox, TN	NO
Monarthrum fasciatum	Knox, TN	NO
Phloeotribus liminaris	Marshall, IN	NO
Pityophthorus lautus	Knox, TN	NO
Xyleborinus saxesenii	Knox, TN	NO
Xyleborus affinis	Anderson, TN	NO
Xyleborus ferrugineus	Anderson, TN	NO
Xylosandrus crassiusculus	Anderson, TN	NO
Xylosandrus germanus	Knox, TN	NO
Bostrichidae		
Xylobiops basilaris	Anderson, TN	NO
Platypodidae		
Euplatypus compositus	Anderson, TN	NO
Oxoplatypus quadridendatus	Anderson, TN	NO
Buprestidae		
Chrysobothris sexsignata	Knox, TN	NO
Cerambycidae		
Neoclytus acuminatus	Knox, TN	NO
Lepturges confluens	Knox, TN	NO

Vita

Tammy Stackhouse was born in Bethesda, Maryland to the mother Natalie Harris. She grew up in Newport, Tennessee where she attended Cocke County High School. After graduation she went to the University of Tennessee, Knoxville where she got a Bachelor's in Science in Plant Sciences with concentrations in Bioenergy and Biotechnology. Tammy started research in bioconfinement in rice and switchgrass before moving to *Geosmithia morbida* research in the laboratory of Dr. William Klingeman, both at the University of Tennessee. Tammy will graduate with a Master's of Science in Plant Sciences with a concentration in Plant Molecular Genetics in May 2019.